Rec'd 11-4-65

PB187391

FINAL REPORT
FOR STUDY OF INFRARED TECHNIQUES
FOR MONITORING STACK GASES

PH 86-65-61

DALMO VICTOR

BELMONT, CALIFORNIA

Reproduced by the
CLEARINGHOUSE
for Federal Scientific & Technical
Information Springfield Va. 22151

A textron company

69

FINAL REPORT

FOR STUDY OF INFRARED TECHNIQUES

FOR MONITORING STACK GASES

PH 86-65-61

Prepared for

Public Health Service, BSS-EH
Washington, D. C.

by

Dalmo Victor Company
Division of Textron Inc.
Belmont, California

October 12, 1965

Prepared by: James M. Lepper, Jr.
Project Engineer
IR Systems

Approved by: J. L. Good
Technical Manager
IR Systems

Approved by: W. A. Porter
Manager
Product Research

R-3159-3954

TABLE OF CONTENTS

		Page
	SYNOPSIS	iii
	Accomplishments	
	Conclusions	
I	INTRODUCTION	1
II	SUMMARY	2
III	CHRONOLOGICAL OUTLINE	3
IV	INFRARED SPECTRAL MEASUREMENT	6
	Equipment	
	Calibration	
	Operations	
	Variables	
V	INFRARED SPECTRA, EXAMPLE	11
	A Detailed Description of the Sequence of Radiative Transfer	
	Theoretical Radiation Sequence Parameters	
	Table of Data for EXAMPLE	
	Radiation Sequence Variables	
	Blackbody Curves	
	Emissivity and Absorptivity	
	Selective Absorption and Emission	
	Linewidth	
	Band Spectra	
	Optical Depth	
	Combined Emissivity	
VI	SPECTRAL ANALYSIS AND COMPARISONS	23
	1. Introduction	
	2. Analysis of Three Targets	
	3. Some Limitations on Feasibility	
	a. Limits due to Plume Constituents	
	b. Limits due to Environment	
	c. Limits due to Equipment	
VII	CONCLUSION	40
VIII	APPENDIX	42
	1. Spectrum Index	
	2. SO_2 Data	
	3. Conversion of Units	
	4. Reference Spectra	
	a. SO_2 Emission, Monsanto #91	
	b. NH_3 with Low Resolution #112	

LIST OF FIGURES

1. Optical Schematics
2. Blackbody Curves
3. Emissivity of Water and Carbon Dioxide
4. Emissivity of Pollutants
5. Combined Emission Curves
6. Atmospheric Transmission and Received Energy Curves
7. Single Scale Spectra of Three Targets
8. Coal Burning Plume and Components
9. Coal Burning Plume with Sky Balance
10. Spectral Averages of an Oil Refinery Plume
11. Range due to Atmospheric Water Vapor

SYNOPSIS

Infrared spectral study of industrial stack plumes was performed to investigate the feasibility of pollution efflux monitoring by remote observation. The study progressed with alternate analytical and experimental work.

Data was obtained by the addition of a telescope assembly to a commercial wide range, high sensitivity infrared spectrometer. The pertinent optical parameters of the instrument were measured with a series of elementary tests aimed at closely approximating the field usage; extended sources at moderate temperatures soon showed that the instrument had adequate sensitivity with only 3" optics.

With the development of suitable instrumentation and operator experience, emission spectral reference tests were performed with heated chambers of varying CO_2, SO_2, H_2O and air mixtures.

A van was fitted with a regulated power supply and shock mounts for remote site operation of the spectrometer. The van was driven to sites in the San Francisco Bay Area, and to a site in Moapa, Nevada.

The recorded spectra show SO_2 densities in different plumes ranging from 50 ppm to nearly 100%.

Over one hundred spectra were run during the course of the study, usually with several traces for each spectrum. Each was analyzed only to the degree necessary to direct the next step in the work.

The conclusions of this study are:

1. Measurement of industrial stack pollution rates is feasible with simple optical systems using common optical components and relatively inexpensive detectors. However, a degree of sophistication is necessary in the electronics to remove the burden of exponential calculations from the operator/analyst. Such computations are amenable to state-of-the-art analog computational techniques.
2. A large number of parameters are significant in reception of radiation from a given plume. For a low temperature process this can result in rather complex organics being generated which tend to clutter the spectra.
3. Pollution densities over 0.3% are readily determined quantitatively for most gases when the plume temperature is over 200° F, when a small to moderate amount of particulate or other gray body radiation is present.

4. Coal burning systems produce a minimum of H_2O vapor which obscures SO_2 to a degree; coal burning power plants are expected to show distinct SO_2 spectra at densities as low as 50 ppm when the particulate exhaust is under control.

SECTION I

INTRODUCTION

This is the final report of the Dalmo Victor Company study and investigation for the Public Health Service, BSS-EH, of infrared techniques for monitoring industrial stack gases, per Contract PH 86-65-61, beginning 2 April 1965. The tasks of this job were to investigate the infrared spectral radiation from industrial plumes, identify certain gases in the plumes by their characteristic infrared signature, and propose, if shown feasible, specific instrumentation and techniques for quantitative emission measurements on a routine basis.

The best way to measure the rate of atmospheric pollution is to observe the source. In the case of large industrial installations causing pollution, direct sampling is done by entering the suspects' premises and disrupting the plant to various degrees by inserting samplers in the equipment or constructing scaffolds to reach the stack exit.

Preferably, an APC agent would merely drive up to the premises and look at the plume. The information obtained by this technique is limited by the narrow range of visable wavelengths within the single octave of 0.4 to 0.8 microns. This investigation covered over four octaves in the region between 2.5 and 30 microns; the region in which molecular characteristics dominate.

SECTION II

SUMMARY

The essence of this report is in four sections; a chronological outline, a section covering the procedures, techniques, equipments, and operations of spectral measurements, an example section which is tutorial in manner but strongly skewed to the problem at hand, and a section with analysis and comparisons of a few of the significant spectra recorded in the course of the project.

Section III covers the events starting with the contract initiation on 2 April 1965. The evolution of the infrared telescope and procedures are described as well as the direction imparted by the analysis of succeeding spectra and attendant theoretical developments.

Section IV covers the sequence of calculation for the determination of the spectral distribution of energy received by a radiometer. The sequence begins with the blackbody curves as a description of the potential energy for radiation. The availability of that potential is the emissivity or absorptivity of the radiating body. The manner in which the emissivity is evaluated and the manner in which the emissivity varies as a function of the engineering parameters is discussed.

Section V analyzes and compares the spectra from plumes of several different processes: a coal-burning power plant, a natural gas-burning power plant, an open-burning natural gas flame, and a malfunctioning petroleum refinery. Pollutants are observed in each of the spectra and estimates of the quantity are made.

SECTION III

CHRONOLOGICAL OUTLINE

The program began 2 April 1965 with assets in each of three primary aspects; theoretical, experimental and operational. Each of these assets was significantly increased throughout the program while the pace of the program was never dominated by any one aspect for more than a week or so. The significant decisions, events and results are abstracted below, while the reasons and explanations for each, if not found in this report, may be found by referring to the appropriate monthly report.

Initial experimental studies were performed with a Beckman IR 5. Since the instrument was not designed as a radiometer, much of the optical data about it had to be obtained by direct measurement. The focal planes were located and the effective aperture and field of view were measured. A number of breadboard optical setups were used to determine a layout which would result in a minimum of instrument modification. Sensitivity measurements were begun using a temperature-controlled extended source.

A month after the contract initiation, some of the optical components which had been ordered began to arrive and accurate measurement of the focal lengths was accomplished. By that time the initial experiments with SO_2 emission in a simulated flue had been completed, showing mainly that greater resolution was required. Thus, an IR 10 was made available and the optical breadboard was retested on the nearly identical optical system of the IR 10. The increase in sensitivity over that of the IR 5 was exchanged for increased spectral resolution.

By the middle of May the basic optical breadboard had been assembled and a short try was made at acquiring local targets viewed from the DV roof. Due to the lack of heavy industry in the immediate locale, the targets proved inadequate; plumes with temperatures on the order of 150°F and only a foot or so in depth rapidly mixed with light breezes and cooled below detection limits.

During the last part of May, a closer approximation of the expected gas density and plume depth was made with a test tank with thermocouple temperature monitoring. Polyethylene windows were used to retain the test gases.

During the month of June, preparations for field trips began in earnest. A small van was prepared with portable power and a shock mount for the spectrometer.

Study of the electronics for means of optimization of the spectrometer with respect to telescopic operation showed that operation as a double beam instrument could be accomplished with the controls in the single beam setting. As a double beam instrument the IR 10 can subtract the energy due to background when the reference beam is aimed at a suitable target. Relative measurements were generally performed with the sky as background reference while absolute measurements required a reference target cooled to a point where it contributed negligible energy.

At the end of June compatability difficulties of the portable power supply and the spectrometer were resolved. Thus, with the addition of the reference optics to the telescope assembly, the system was ready for field trials.

The first trips had a low level of success until the limits of range, weather and target dimensions were worked out. Continued testing with a larger test tank (18" dia.) was done to correlate the field of view and range effects found in the field. The weak bands of CO_2 at 9.4 and 10.4 microns were observed with the test tank first then confirmed in the quite successful spectra run at the Hunter's Point Pacific Gas and Electric thermal power station.

Study of the PG&E spectra in early August showed the anticipated water vapor interference with the 7.3 micron SO_2 region, but showed a strong interference in the region of the 8.7 micron band as well. Numerous runs were made to evaluate the degree of the overlap, both in the test tank and with field trials.

Recurrent efforts were made to locate large coal-burning operations in western United States. Finally, near the end of August, it was found through communication with coal companies that the farthest west operation of any consequence was the Nevada Power Company's plant on an Indian reservation in Moapa, Nevada.

In preparation for the trip, 16 spectra were run of Tidewater Oil Company's fluid coker. The plume from the coker appeared to be the closest to that anticipated at Moapa; i.e., lower in water vapor and higher in SO_2 and particulates than any of the other industrial plumes in the Bay Area. A pure hot SO_2 plume from Monsanta Company's sulfuric acid plant was observed on the same trip, giving a measure of the long range attenuation of SO_2.

August ended with the successful trip to Moapa. The stack at Moapa is 200 feet high with a large volume flow at about 320°F. The first day of measurements were conducted in moderately high winds with attendant disruption of the signal. Scanning began on the second day early in the morning before the usual desert winds developed. Six scans were made at a range of

about 700 feet. Due to the rigors of the trip, the gain of the system was reduced by a factor of two or three, lowering the signal to noise ratio. However, enough scans were made to allow averaging which, in turn, restored a useful signal to noise level to the records. There was also noted an increase in noise in the SO_2 band compared with adjacent spectral regions. Background effects were significant due to the large amount of ash in the plume, so a certain degree of black body compensation was applied by reducing the reference window aperture. The resultant SO_2 density was determined to be approximately 500 ppm.

The experimental series ended with the measurement of radiation from a test flue burning hydrogen, a check on the strength of water vapor lines appearing in the regions overlapping SO_2, NO_2 and CO_2 spectra.

The last part of September was spent in preparing data for the final report.

SECTION IV

INFRARED SPECTRAL MEASUREMENT

Data was gathered from three sources; (1) a search of pertinent published data was made, (2) and correlated with data from test setup measurements with known conditions, (3) these data were then correlated with those taken in the field. The equipment and techniques are described below.

1. Equipment

A sensitive, wide range grating spectrometer, the Beckman IR-10, was converted to a passive, compensated, telescopic spectrometer by the addition of a simple reflective telescope and beam routing mirrors. The IR-10 normally operates as a double beam spectrometer in the IR range of 2.5 to 33 microns wavelength, or 4000 to 300 wavenumbers. The energy from a hot IR source is directed by a pair of focusing-mirror sets into a reference and an analytic beam through a sample compartment. The ratio of the energy in the analytic and reference beams is taken with an optical balance technique where an attenuator is moved into the reference beam to balance losses in the analytic beam. The beams are alternately fed by a chopper mirror into the bandpass filter and diffraction-grating monochrometer. The monochromatic signal is detected by a thermocouple. The signal is amplified, and the AC component, proportional to the imbalance of the two beams is fed back to the attenuator servomotor. The attenuator position as a function of wavenumber is then recorded as percent transmission versus wavenumber (frequency).

In Figure 1, the telescope installation on the IR-10 is sketched. For the telescopic measurements the beams from the internal IR source are blocked, and the line of sight out of the monochrometer is redirected to a 3" first surface spherical mirror. The line from the spherical mirror to the target is directed by means of a gimbaled flat mirror. The gimbaled mirror is large enough to accommodate the beam from the 4 power sighting telescope as well.

The line of sight for the reference beam is redirected to the gimbaled mirror without benefit of the focusing mirror. The unfocused reference beam allows the narrow analytic beam to be compared with a broad averaged region to the right of the analytic line of sight. Energy from the background may thus be subtracted from the target energy.

Since the servo-operated attenuator is not in this sequence, the feedback is accomplished with internal electrical signals. The accuracy of the measurement is no longer guaranteed by the attenuator characteristics and calibration is necessary to compensate for the variations in the effective gain of the filters, gratings, and thermocouple.

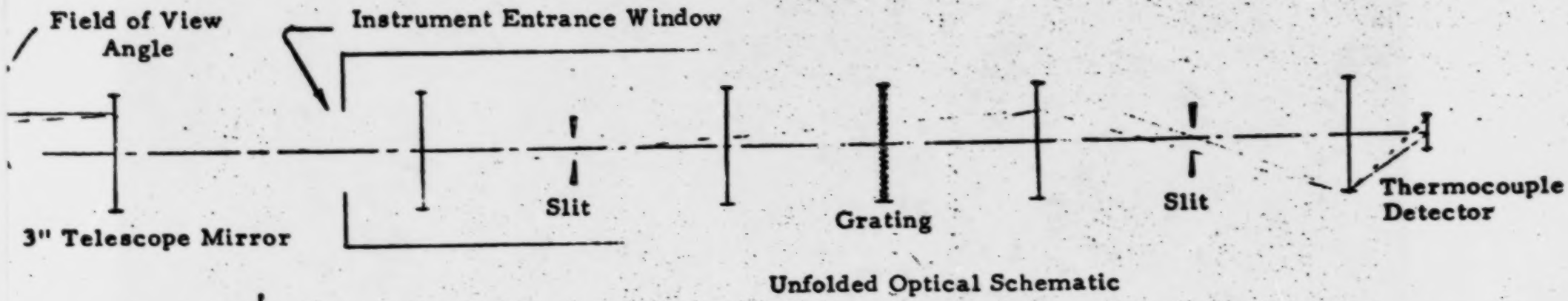

Unfolded Optical Schematic

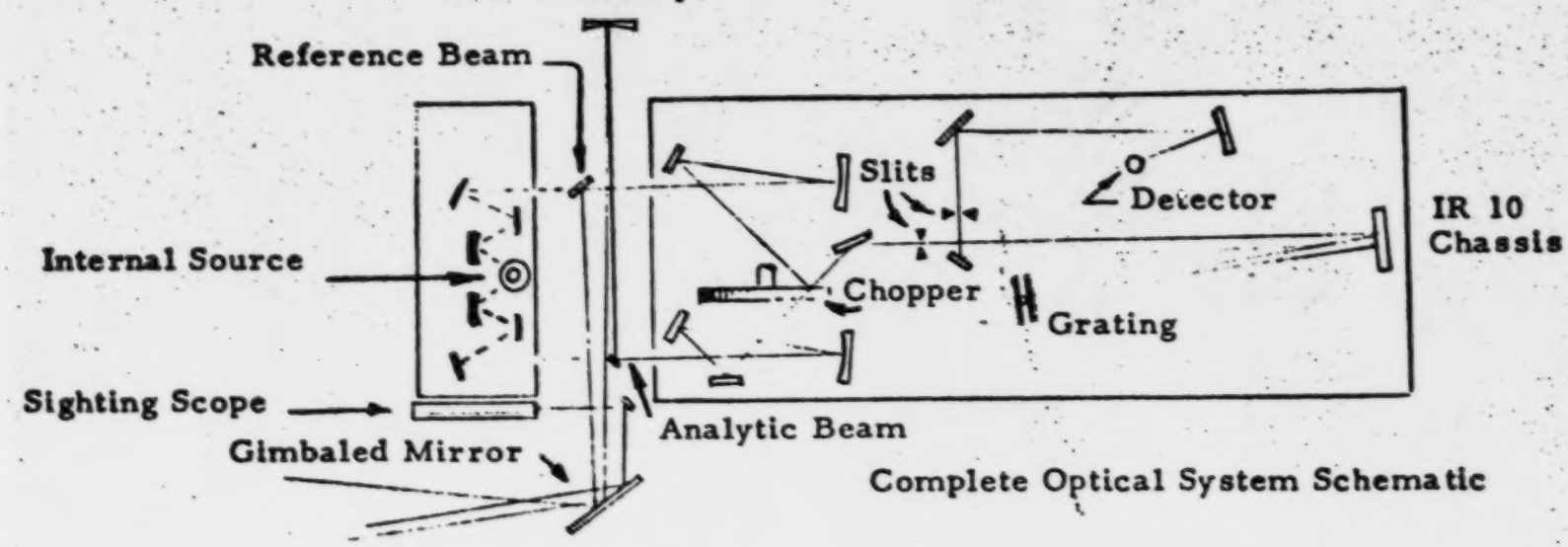

Complete Optical System Schematic

FIGURE 1

Optical Schematics

It is desirable to gather as much energy as possible since signal gain above a certain minimum may be traded for spectral resolution. Originally a 12" aperture telescope mirror was anticipated in view of the low energy levels from targets below incandescent levels. However, the nature of the optical sequence in the monochrometer requires an optical relay; i. e., a series of focusing and refocusing mirrors. As seen in the optics sketch of Figure 1, the field of view of the detector down the optical path is limited by several apertures and is analogous to the narrow field of view of periscopes. Only gross modification of the spectrometer would allow an effective aperture greater than 3". Since the spectrum controlling slits are in image planes the final field of view looks like a slit, approximately one degree high and less than a tenth degree wide. For the reference beam, the field of view is an unfocused region nominally 5 degrees in diameter.

Further concentration of the beam could have been made with a cylindrical parabola bringing the final dimensions close to a 0. 1 degree circle. Although tests were made with a breadboard system, the cylindrical element was dropped because it was felt that the linear field of view would provide a means of keeping wandering plumes in the field of view while not suffering the loss due to a large, round field of view.

If the field of view is small and the target always fills it, then the signal loss with range is mainly a function of atmospheric attenuation. If the field is a line which cuts through the target, then the loss is approximately linear with range. If the field is larger than any target dimensions, signal loss increases not less than with the square of the range.

A recorder was available to perform continuous monitoring of selected wavelengths. In practice, it was not so useful. Variation in the plume intensities is obvious from the noise level of the spectrograms; further, it is desirable to make relative intensity measurements, rather than attempt absolute measurements at a single frequency.

The equipment was mounted on a van on a special shock mount structure and powered by lead-acid batteries through a DC to AC inverter with accurate voltage and frequency control.

To predict and confirm field measurements, test chambers and flues were erected. Typical flue gasses were introduced singly and in combination, heated and observed with the spectrometer at varying ranges.

The test chambers were 36" long and initially 8" in diameter while later tests were with an 18" chamber. One half mil polyethylene windows were used which limited the temperature to about 255F. Though polyethylene melts at 230F, the windows survived the chamber temperatures due to the high chamber-to-atmosphere temperature

gradient through the thin film. The polyethylene did not obscure the spectra since the thin film has only weak bands at 3.5, 7 and 14 microns. The gasses were stirred with a fan and monitored with two or three thermocouples to assure uniformity. Fifteen degree gradients were typical. A flue with unglazed windows was set up for higher temperatures. It consisted of about 12 feet of 8" stove-pipe connected horizontally with both ends open to the spectrometer line of sight. Gasses from the burners entered about 4' from one end, traveled horizontally about 4' then went up a short stack. The unused sections at each end served to impede flow out the open windows.

The gasses studied in the test set-ups were H_2O, CO_2 and SO_2. Nitric Oxide (NO) was available, but not used due to its extreme toxicity. Concentrations as found in flues of only 200 to 700 ppm are fatal, and symptoms of damage may not appear for periods up to 72 hours.

2. Calibration

An exact thermal calibration was never performed with the IR-10 telescope. To make such an exact measurement would require a large area source of known spectral power density. The size is necessary because of the field of view of the system when the telescope is used. A calibrated source of kilowatt power capability was not located or built. However, it has not been necessary to have an exact calibration of the thermal sensitivity since the primary measurements have been relative to each other. In most cases of field measurement, the plume has not been visable whatsoever and as a consequance, only an upper limit of the energy density of the target may be made. Received energy varied in field trials over a range of five decades due to the large number of variables. Wavelength calibration is not a problem since nearly every spectrum run has some landmarks, usually CO_2 or H_2O.

3. Operations

Suitable targets for field trials were located through the help of the Bay Area Air Pollution Control District. The Bay Area Air Pollution Control District has been very thorough in its operation, and supplied considerable data with respect to the physical dimensions, temperatures, and pollutant densities for those few sources remaining in the Bay Area. A measure of their effectiveness in pollution control is the two hour drive necessary to locate any significant sources.

Certain restrictions due to the weather had to be observed; visability restrictions are obvious. Not so obvious was the degree to which an invisable plume was being bent over and mixed by the wind. Generally, winds in the 20 to 30 knot range produced too much mixing and attendant cooling. However, pollution is not too significant in a 20 - 30 knot wind.

The absolute humidity is important in spectral measurements since water vapor is the most significant absorber in the signal path. Although the relative humidity varies considerably during the day, the absolute humidity changes quite slowly under fair weather conditions. The common measure of this parameter is dew point, and data is readily available around the Bay Area from the airport weather stations as hourly records. The dew point for the time of a spectral scan is then converted to precipitable centimeters of water per kilometer for spectral attenuation calculation.

The relative humidity is of importance only when the ambient temperature approaches the dew point. Then haze, fog or other distributions of water occur which depend on the recent history of the specific air mass and the amount of Aitken particles present (transient condensation nuclii on the order of 0.1 microns dia.). The condensed particles then skew the received spectra by combinations of scattering and broad spectrum attenuation effects.

4. Variables

There is a large number of variables associated with each spectrum, some of which vary during the recording. Even with the calmest of wind conditions, a plume with enough heat to be observed will rise rapidly and create its own turbulent mixing. This, in turn, significantly modulates the received signal. To resolve the signal, several records are made and averaged.

In the case of the coal burning stack at Moapa, the plume appeared steady and vertical to an altitude of several hundred feet. However, the stack is 200' high with an exhaust velocity on the order of 60 ft/sec. This means that the Reynolds number (inertial force/viscous force) is several orders of magnitude above the turbulence threshold. Thus, the exhausted gasses begin to rapidly mix with the cool air in the form of large distinct vortices shed by the hot core of the plume. In turn, this caused signal variation on the order of 20 to 30 percent.

Further variation occured, evidently due to variations in the SO_2 density. The data in the 8.7 micron region of the spectra (SO_2 band) show half again as much noise as in the immediately adjacent region around 8.3 microns. Since the SO_2 is essentially a trace element in the coal, its density is expected to vary more than that of the major constituents like CO_2. In that case, averaging of data spread over one or more days will give a more realistic measure of the pollution rate.

System load variations become a significant parameter when observing power stations. The load variation of the Hunters Point Pacific Gas and Electric station caused 4:1 signal variations in spectra run at different times. In that case, averaging would not be desirable; rather an independent set of calculations using ratio measurements are necessary to account for spectral changes.

SECTION V

INFRARED SPECTRA, EXAMPLE

1. General

To introduce the spectra taken during the various field trips, an example is calculated showing the sequence of energy transfers which control the energy received in a given situation. This example will then be compared with the actual measurements. Before each step in the example, a theoretical description of the process is given.

2. Theoretical Radiation Sequence Parameters

For example, a large coal burning steam power plant exhaust plume is studied. Values for parameters were taken from typical stacks, and within the normal ranges of those parameters, convenient values were chosen, such as the stack diameter of 5 meters (16' 5").

The complete listing of the parameters assumed is in Table 1.

Detailed calculation of the radiation from a continuously varying temperature gas cloud is beyond the state of engineering calculations; thus an arbitrary boundary layer was assumed to illustrate the significance of the non-uniformity. Most large stacks supply a boundary of cool air within the stack which mixes to a certain degree providing a cool radiation shield at the wavelengths of greatest absorption. Because of atmospheric absorption playing a similar role, the boundary layer has only a small effect as will be seen below.

The temperature of the gas plume has a significant effect on the gas density used for computation. Since most of the gas is nitrogen, a simple application of the formula PV= RT (pressure times volume equals a constant times the absolute temperature), yields the correction factor for all the gases except H_2O. Since the H_2O is near its boiling point, the temperature-density function is more complex so values were taken from standard steam tables for the exact temperatures used.

3. Radiation Sequence Variables

Black Body Curves. Figure 2 gives the black body radiation curves for the pertinent temperatures of the example. The black body curves give the radiated energy density as a function of temperature and wavelength for a heated body which has a uniform maximum radiation efficiency at any wavelength. Thus the distribution of radiated energy is a function of the temperature only and not of the specific radiator. A black body absorbs all energy incident upon it, and in turn, radiates energy as a function only of its geo-

TABLE I

This table lists the assumed values used in the calculations of stack plume example. The example is a general illustration and the gas concentrations used do not necessarily represent a particular fuel.

Assumed Plume Dimensions	
Diameter	5 meters (16' 5")
Boundary or Mixing Layer	8% of Diameter, 40 cm (16")
Effective Core Diameter (Due to low density at 300° F)	3 meters (10')
Effective Boundary	10%, 30 cm (12")
Effective Core Diameter for H_2O (calculated from steam tables)	4.2 meters at 300° F
Effective Boundary for H_2O	0.4 meters at 188° F
Temperatures	
Core	420° K (300° F)
Boundary Layer	360° K (188° F)
Ambient	76° F
Background Minimum (Stratosphere)	220° K (-70° F)
Range (from stack plume to instrument)	300 meters (1000 feet)
Gases in Path	
CO_2 (at 320 ppm natural level)	9.6 atm-cm
H_2O in Path (at 56° F dewpoint)	4 mm
Gases in Plume	
CO_2, 3 m at 13%	39 atm-cm
0.3 m	3.9 atm-cm
H_2O, 4.2 m at 12%	2.2 mm
0.4 m	0.21 mm
SO_2, 3 m at 1000 ppm	0.3 atm-cm
NO, 500 ppm initial concentration assume 20% conversion to NO_2 in the boundary (mixing) layer	0.15 atm-cm at 300° F
	0.012 atm-cm at 188° F
NO_2 from NO, 100 ppm in boundary	0.003 atm-cm at 188° F
CH_3COOH at 300 ppm	0.1 atm-cm

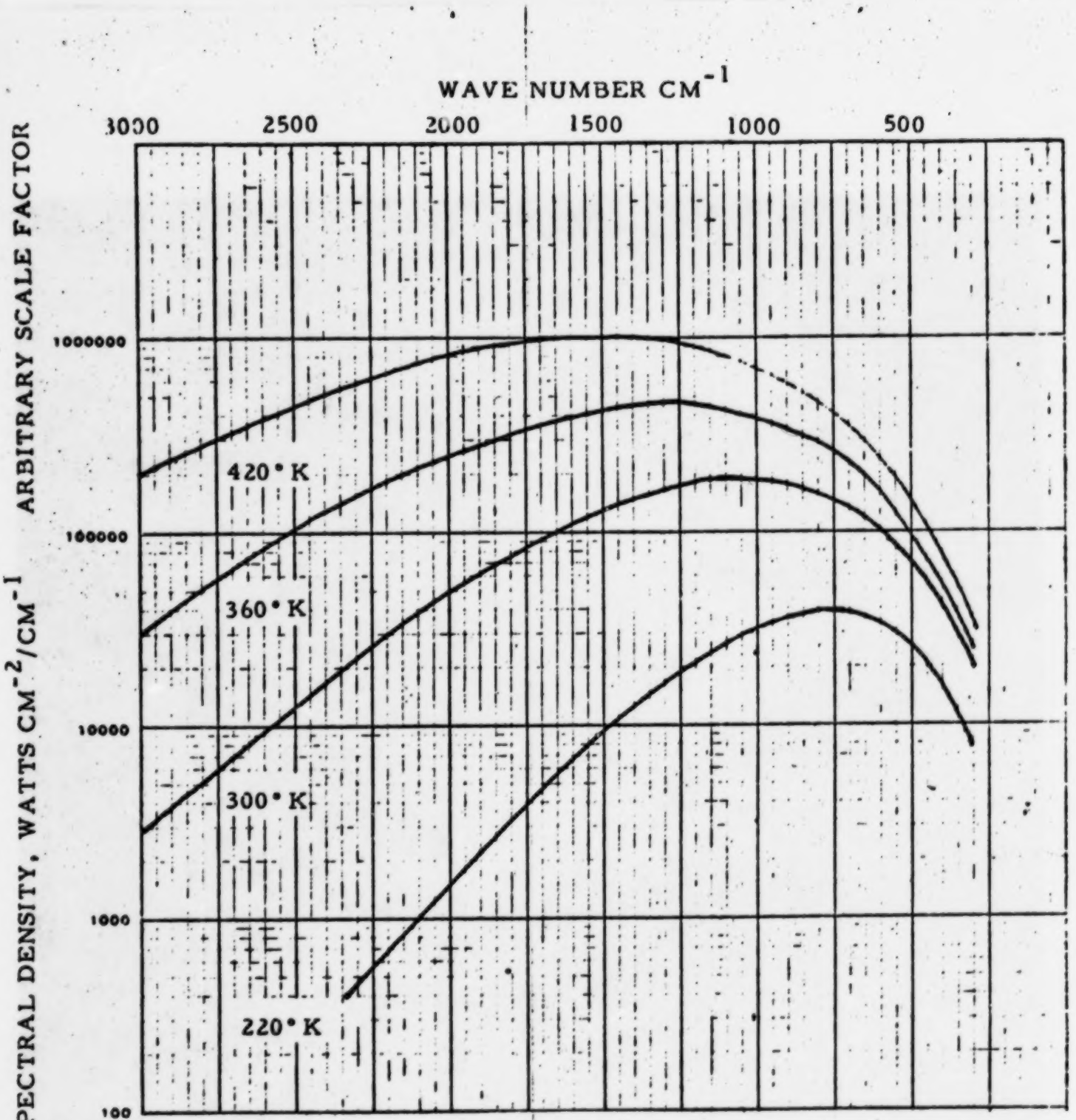

FIGURE 2

Blackbody Energy Density Curves for Temperatures of the Detailed Example

metry and temperature. The function may be described as

$$R^{\circ} d\lambda = \frac{c_1}{\lambda^5} \frac{d\lambda}{[\exp (c_2/\lambda T]-1}$$

where $R^{\circ} d\lambda$ is the radiation density in units of power per unit of wavelength,

T is the absolute temperature,

c_1 and c_2 are constants depending on the system of units used, and λ is the wavelength.

The black body curve may be considered as the potential of a body to spontaneously radiate a given wavelength. When two bodies are the same temperature they radiate equal amounts of energy to each other, and no net exchange occurs. At different temperatures the average of exchanged energy favors the lower temperature.

Emissivity and Absorptivity. A measure of the impedance to radiative transactions is the emissivity of a body. Except in the case of stimulated emission (as in a laser) the emissivity of an object may be considered identical to the absorptivity. If a high temperature black body is placed behind a relatively cool gas cloud, and the decrease in received energy is 30%, then the absorptivity is simply 30%. But if the cloud has a temperature equal to that of the source previously used, then it will not only absorb 30% of the incident radiation, but emit at 30% of its potential rate, exactly compensating for the loss seen by the detector. Therefore, the gas cloud effectively disappears, and its presence or absence cannot be ascertained by its radiation.

Selective Absorption and Emission. The point of this contract is that gas clouds do not absorb or emit radiation as uniform functions of wavelength. There are a number of physical phenomena that are selective functions of wavelength, but the cases at hand are dominated by the vibrational characteristics of the gas molecules in question. These vibrations and their stronger harmonics occur in the range of frequencies studied with the IR-10. The vibrating molecules, if they have a permanent dipole moment (asymetry of electrical charges) act as transmitting or receiving antennas, and absorb or emit according to their thermal potential at the vibrational frequency. Symetrical molecules such as H_2, N_2 and O_2 do not interact in the infrared region, but their vibrational frequencies may be observed as modulation of beams through them at other frequencies (Raman effect).

The vibrating frequencies are determined by the bond strength and the masses of the atoms of the molecule, and then are modulated by the rotational and translational velocities of the molecules. The

molecules may rotate only at integeral rates, described by quantum mechanics. This results in the vibrational lines being divided into uniformly spaced (in frequency) fine structures of a band. The envelope of the band of lines is determined by the statistical distribution of rotational energy for each vibrational mode. Modification of the fine structure occurs as the width of the individual lines changes.

Line Width. There are three significant phenomena which broaden the individual lines of a vibrational band: Natural, Collision, and Doppler broadening. When the temperature of a gas is below the incandescent level and the pressure is atmospheric, collision broadening usually dominates.

Natural broadening is the absolute minimum line width due to uncertainty in the energy transition levels, and is analogous to Heisenberg's uncertainty principal in derivation. Doppler broadening is due to the random motion of the gas molecules with a resultant gaussian shape. Collision broadening refers to the perturbations caused by collisions among the molecules, and is an inverse function of the mean time between collisions, and the damping coefficient for the radiating molecule. Since the mean time between collisions is a function of pressure, pressure broadening is referred to.

The half widths, where the emissivity is one half that of the line center may be described as follows:

$b_n = 1/4\,\pi\,c \quad (\gamma_u + \gamma_l)$

$b_c = 1/4\,\pi\,c \quad (2\,z_u + 2\,z_l)$ proportional to $T^{-1/2}$

$b_d = \left(\frac{2KT\,\ln 2}{mc^2}\right)^{1/2} \omega_{ul}$ proportional to $T^{+1/2}$ and frequency

where u and l refer to the upper and lower energy states associated

with the before and after conditions of a photon exchange,

K is Boltzmann's constant

and where c is the speed of light

γ is the damping coefficient
$1/Z$ is the mean time between collisions
and m is the mass of the molecule involved.
ω is the frequency of the line center

The wings of the individual lines may overlap, and indeed, under high pressure the lines may disappear entirely, leaving a simple contour to describe the vibrational bands.

Band Spectra. Figure 3 gives the emission spectrum for the gases H_2O and CO_2 which are the major emitters in stack gases. The effect due to the quantity will be described below. Consider CO_2 for an example of the salient features of vibrational bands. It is a linear symetric triatomic molecule which can have three fundamental modes of vibration. These occur at frequencies (wavenumbers) of 667.3, 2349.3 and 1340 cm^{-1} or wavelengths of 15, 4.25, and 7.46 microns. They are referred to as ν_2, ν_3 and ν_1 respectively. The last of these, ν_1, does not interact in the infrared and is a Raman line. The combination of these three fundamentals and their harmonics yield over 43 weaker bands, many of which overlap or are contiguous. The combinations $\nu_3-2\nu_2$ and $\nu_3-\nu_1$ are weak but important bands centered at 9.4 and 10.4 microns. Radiation from the stronger CO_2 bands is strongly absorbed by atmospheric CO_2 while the emission from the weaker bands is barely effected.

Optical Depth. For quantitative measurements the manner in which absorption increases with increasing numbers of absorbing molecules, or equivalently the path length into an infinite cloud necessary to produce a specified amount of attenuation is studied. If a gas absorbs a certain percentage of the incident radiation per unit length, the percent transmission of the whole may be simply described in the form of Beer's law; percent transmission T is equal to B^{-px}, where B is a suitable logarithmic base such as 10, e, or 2, p is the partial pressure or similar concentration factor, and x is the total pathlength. A scale factor is chosen to suit the logarithmic base.

Such an exponential calculation is simple if the emissivity is calculated for one given wavelength. However, if a salient line structure is present, either detail incremental calculations must be made or a more general formula used. An exact solution in closed form is not available, but three statistical approximations are in common use: the Goody, Elsasser, and King (universal) models. The exact number and location of fine structure lines in a band is not of great consequence in low resolution studies like the present one, therefore in the models the important parameter is the line shape which is essentially identical for each line except for a scale factor. In the Elsasser model all lines within a band are considered equally spaced and of uniform intensity. The Goody model considers random spacing and random intensities, while the King model covers both cases with a variation of parameters. Two elementary solutions appear for the limiting cases of weaklines and strong lines. At low optical densities a linear relationship holds, as with Beer's law, where doubling the number of absorbers simply gives twice the absorption. In the case of strong lines, where all the energy at the line center is absorbed near the beginning of a path, the energy transmitted at frequencies between the lines is absorbed

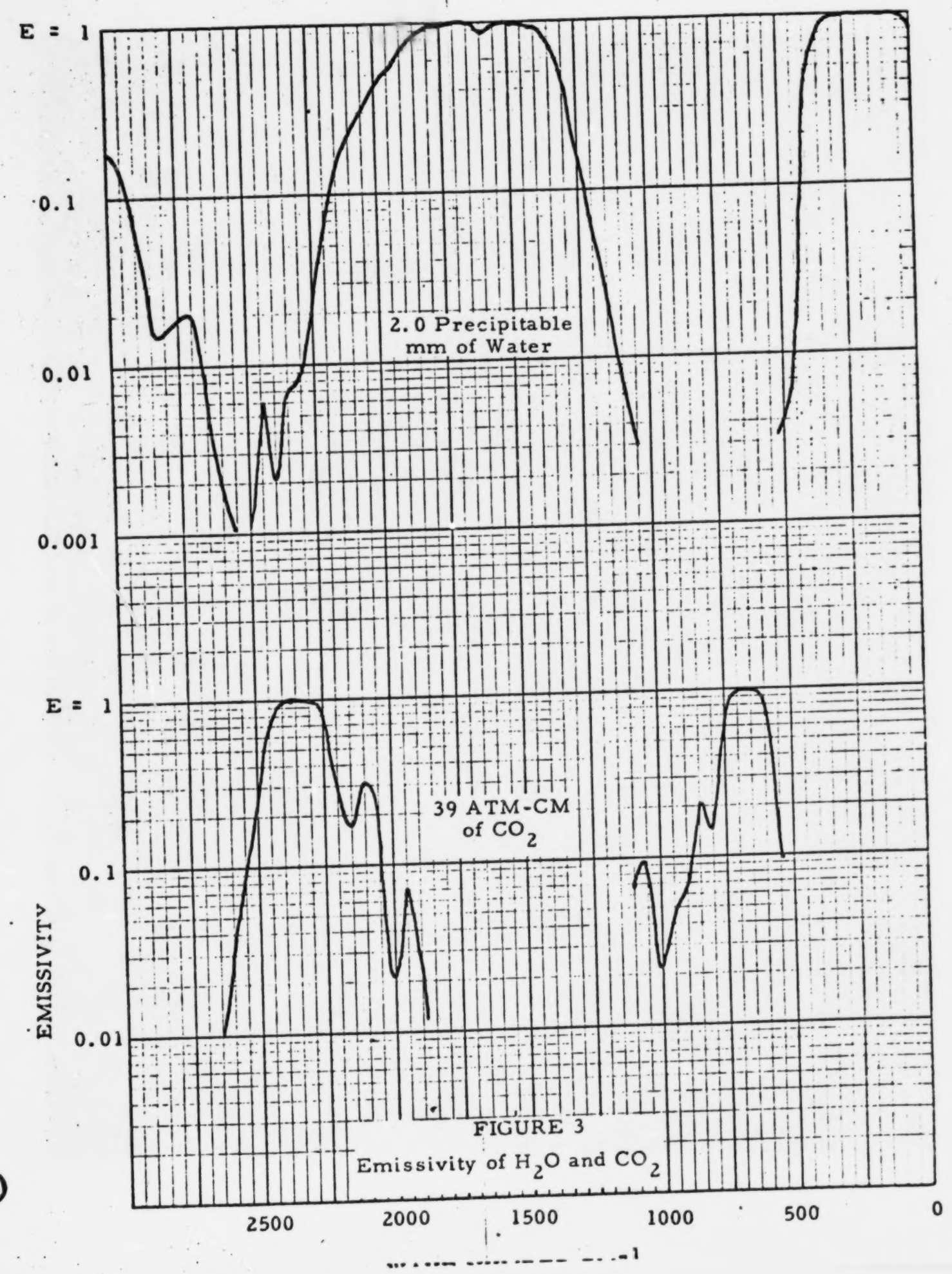

FIGURE 3

Emissivity of H_2O and CO_2

in proportion to the square root of the number of absorbers.

For the present example the data was taken from computer calculated tables using a random Elsasser model which agrees with H_2O and CO_2 measurements. For the pollutants, little data was available, and the calculations were based on Beer's law interpolation and extrapolation of experimental and published measurements. The spectral intensity of the pollutants is shown in Figure 4 for the gas densities from Table 1.

Combined Emissivity. The combined effect of the example flue gases and pollutants is shown in Figure 5. The curve is the product of all the appropriate transmission factor s without regard to complex fine structure. This approximation is good where the total emissivity is small, while in the denser spectral regions resolution of the components is unlikely in actual measurement, thus unimportant here.

The second curve of Figure 5 illustrates the product of the associated black body curves and the emissivity curve, the dashed portion showing the effect of the cool boundary layer in the regions of high spectral density. The units of intensity are arbitrary since it is a matter of the geometry of the situation and optics, and incidental to the radiation sequence.

The third curve of Figure 5 is the reference as seen by the instrument. It illustrates the energy received from the sky background and was derived by taking the atmospheric transmission function (the curve at the bottom of the figure) and fitting it between the black body curves of the ambient temperature and that of the stratosphere. As the optical depth of the atmosphere increases, the average line of sight extends to greater altitudes along the slant path past the target plume. A suitable temperature for a major portion of the stratosphere is 220K, such a low value that its energy contribution need not be measured with great accuracy.

Atmospheric Attenuation.

Since the atmosphere contains the same major constituents as the radiating plume, it absorbs primarily in the regions of emission. As a consequence, most of the energy emitted is absorbed before reaching the instrument.

The atmosphere contains, besides the infrared inactive nitrogen and oxygen, carbon dioxide, water vapor, and trace amounts of HDO (heavy water, 280 ppm) N_2O, O_3, methane, and variable amounts of industrial pollutants such as SO_2 (0.01 ppm background, 0.1 ppm in industrial regions with 0.5 ppm concentra-

```
1000   I
1350   +
0.7407 A0
1000   B1
1150   +
0.0006 A0
1000   I
       B+
1.0000 A0
1000   B1
       B1
1150   +
0.8695 A0
       B1
 520   +
1.9230 A0
10000  B1
       I
1850   +
5.4054 A0
       B1
1280   +
7.8125 A0
       B1
 750   +
13.3333 A0
       B1
2150   +
4.6511 A0

       B1
 667   +
14.9925 A0
       B1
2300   +
4.3478 A0
       B1
1900   +
5.2631 A0
       BS
100000,81
       B1
1100   +
```

	λ μ	ν cm^{-1}	cm path for $\epsilon = 0.1$
CO_2	4.25	2349.3 (ν_3)	
	7.46	1340. (ν_1)	
	15.	667.3 (ν_2)	
$\nu_3 - 2\nu_2 \approx 9.4\mu$			
$\nu_3 - \nu_1 \approx 10.4$			
SO_2	7.407	1350	.0263
	8.695	1150	.10
	19.230	520	.30
NO	5.405	1850	.632
NO_2	7.813	1280	.033
	13.333	750	.055
CO	4.651	2150	.09

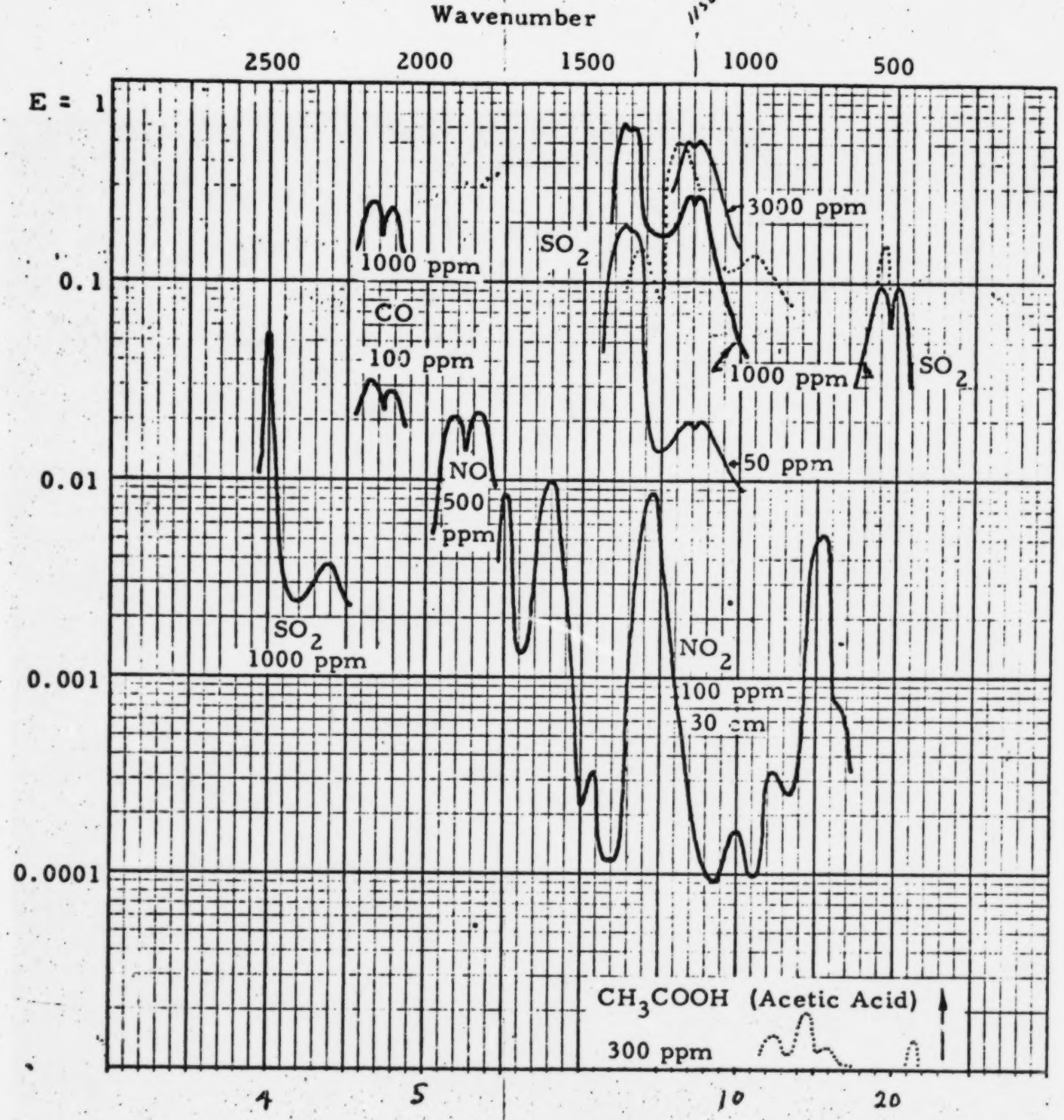

FIGURE 4

Emissivity of pollutants at typical relative molar concentrations (parts per million) for a 3 meter effective path (NO_2 at 30 cm)

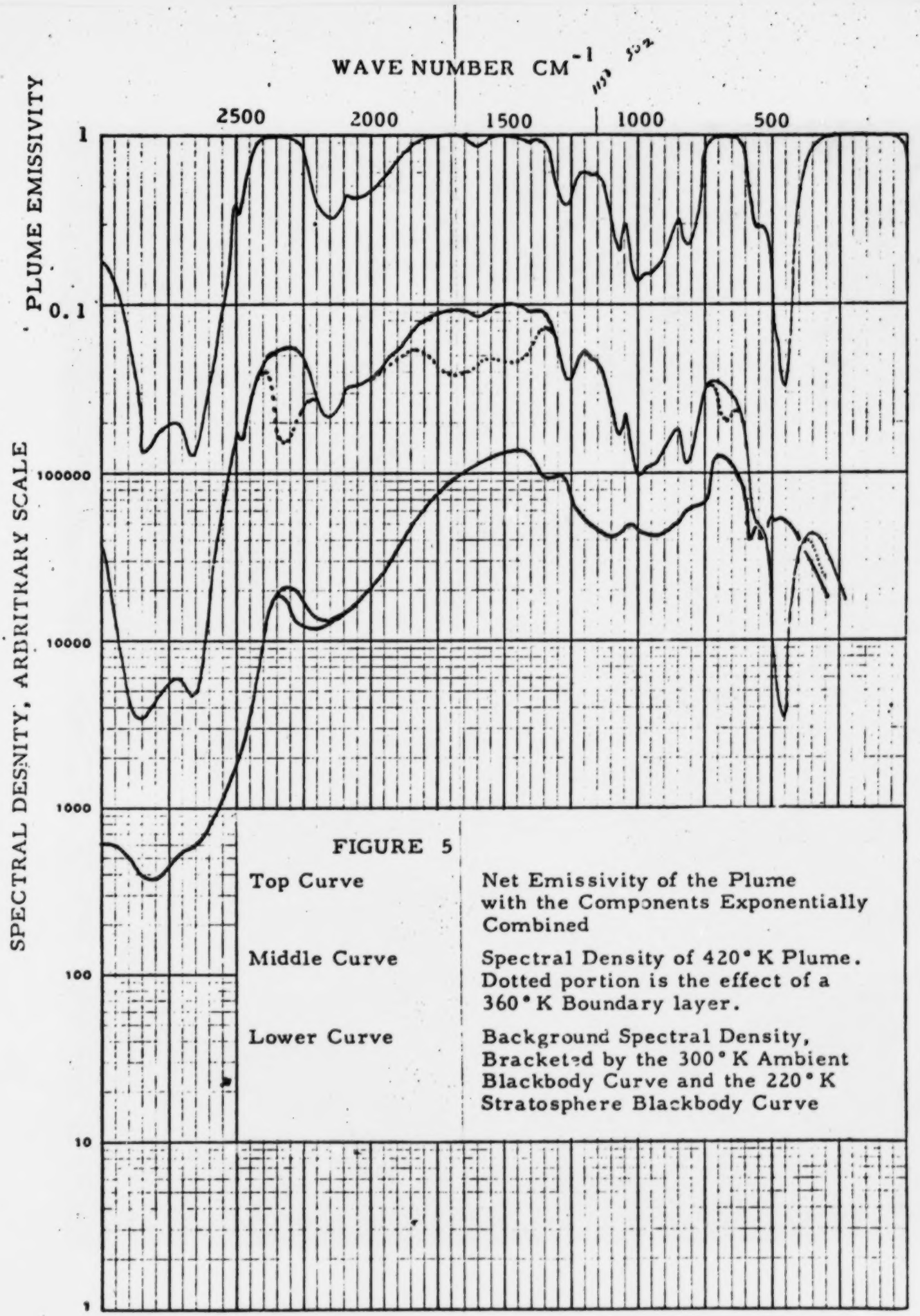

FIGURE 5

Top Curve	Net Emissivity of the Plume with the Components Exponentially Combined
Middle Curve	Spectral Density of 420° K Plume. Dotted portion is the effect of a 360° K Boundary layer.
Lower Curve	Background Spectral Density, Bracketed by the 300° K Ambient Blackbody Curve and the 220° K Stratosphere Blackbody Curve

tions and 2 ppm transients are typical) and automobile pollutants such as CO. At a range of 300 meters, the spectra of N_2O and HDO are barely discernible. Ozone may have a specific absorption on the order of 10% during maximum concentrations though ordinarily it and the other trace gases will not be significant. Carbon dioxode normally runs 320 ppm ±10%, but in industrial regions such as Los Angeles the level may be three or four times as great. The effect of water vapor variations has been discussed above under weather variations.

The combined effect of the atmospheric constituents illustrated at the top of Figure 6 was derived from the actual measurements at 300 meters of Taylor and Yates to account for any trace effects not isolated, with compensation for the water vapor concentration assumed in the example.

Received Energy. The total energy received appears in Figure 6 with the shaded portion being the balance when the reference energy is subtracted automatically by the instrument. The magnitude of the reference correction is small in this case, but in the case of low density plumes, the low temperature of the background is a dominant factor causing the instrument to head toward negative read out values and run against the stops. The proper balance of energy is obtained for cases where particulate matter in the plumes cause the addition of black body radiation when the reference aperture is obscured with by a compensating amount of black body. In practice a piece of cardboard will suffice, though a better balance would be achieved with a heated reference attenuator (where the spectral details of the attenuator would become important).

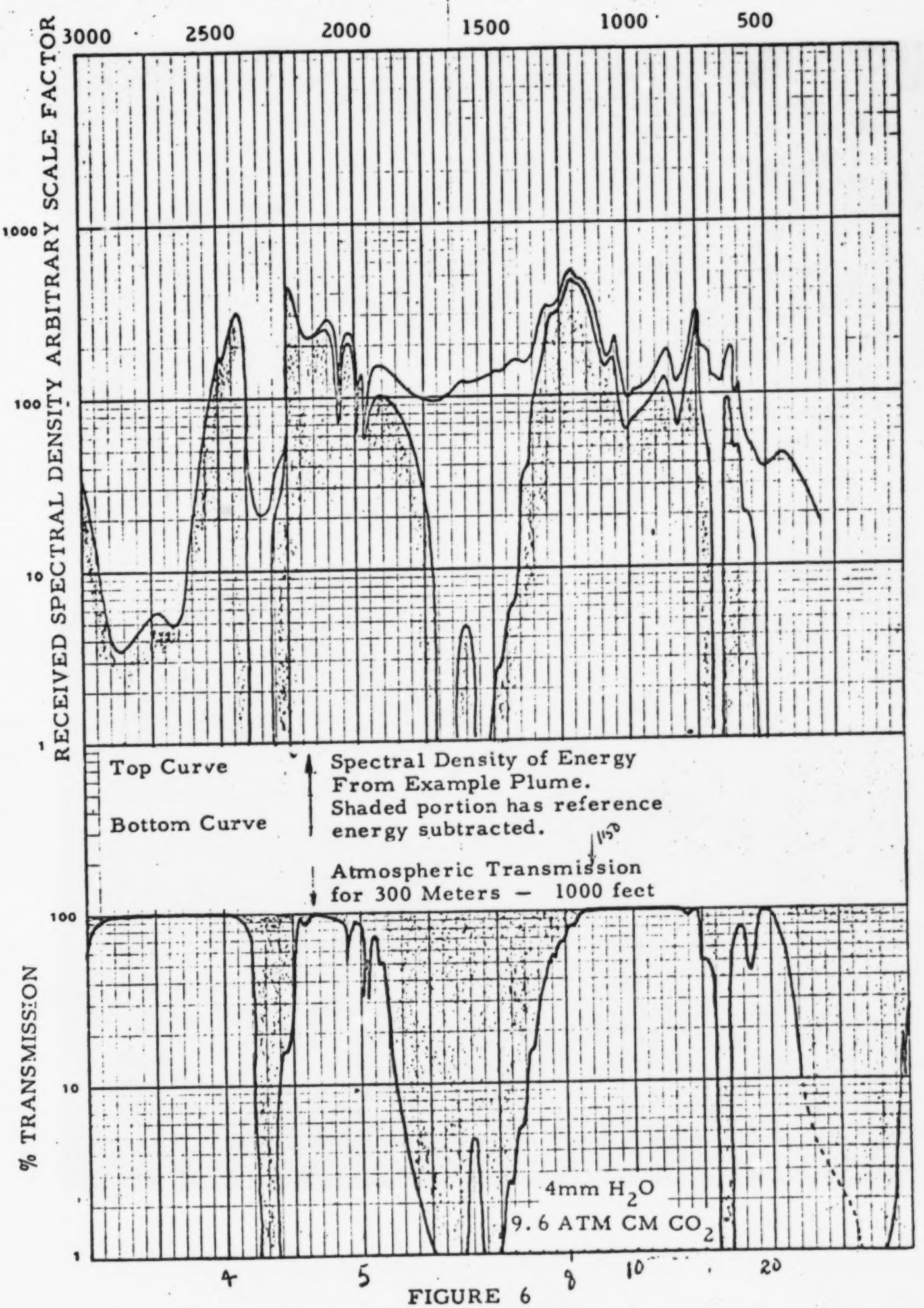
3000
2500
2000
1500
1000
500
RECEIVED SPECTRAL DENSITY ARBITRARY SCALE FACTOR
1000
100
10
1
Top Curve
Bottom Curve
Spectral Density of Energy From Example Plume. Shaded portion has reference energy subtracted.
Atmospheric Transmission for 300 Meters — 1000 feet
% TRANSMISSION
100
10
1
4mm H_2O
9.6 ATM CM CO_2
4
5
8
10
20

FIGURE 6

SECTION VI

SPECTRAL ANALYSIS AND COMPARISONS

1. INTRODUCTION

The purpose of the spectral analysis is the quantitative determination of the pollutant flux in the observed (radiometrically) plume. In the following we consider first what pollutants are of primary interest (SO_2 etc.), what we expect the spectrometer to see (extrapolation and interpolation from the example computed), and finally an analysis of what was actually seen by the spectrometer.

The choice of what to look for in the spectra comes from two sources; the pollutants specifically pointed out in the contract as significant, and those discovered in the search for a complete accounting of the exhaust components of a particular process. Thus the analysis considers the quantities expected of oxides of sulfur, nitrogen, and carbon, and a check of the results of intermediate products of combustion being swept out the exhaust: ammonia, (NH_3), acetic acid (CH_3COOH), hydrogen sulfide (H_2S), and cyanogen (CN_2), for example.

What is expected in the spectra is first a general distribution of the energy associated with the blackbody curve of the plume temperature; second, the "shadow" of the atmosphere between the target and detector; third, the major constitutents of the plume associated with the process (generally burning), and fourth, the details of the spectrum created by the relatively small amounts of pollutants being sought. Since generally the pollutants contribute only a small amount of the total energy detected, a considerable amount of comparison work is performed to be certain that the details are not just minor functions of the major constitutents of a plume. Once these determinations are made the process is routine and applicable to automatic analysis.

In the actual application of the analysis, the final and most important step, then, is the actual observation and measurement of the pollution after the effects of environment, and process are accounted for. In the actual use of the final instrument the operator's degree of understanding of the system will be balanced against the complexity of the built-in signal processing equipment.

2. ANALYSIS OF THREE TARGETS

Three targets are compared with the example of the preceding section in the following. The spectra of the three are presented in Figure 7 . Because of the large number of significant parameters describing each of the spectra, a simple two dimensional display

K•E SEMI LOGARITHMIC 358-94L

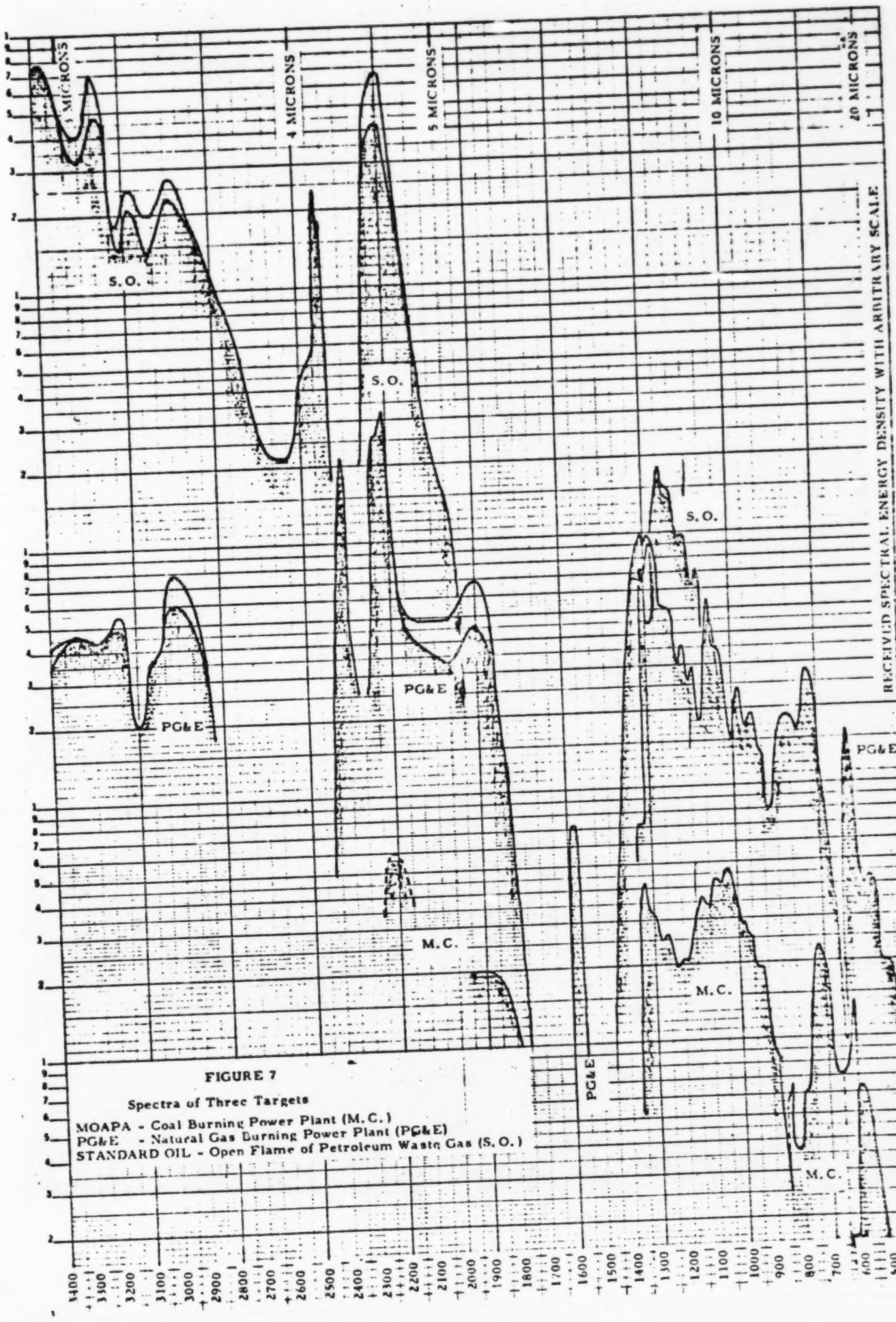

FIGURE 7

Spectra of Three Targets

MOAPA - Coal Burning Power Plant (M.C.)
PG&E - Natural Gas Burning Power Plant (PG&E)
STANDARD OIL - Open Flame of Petroleum Waste Gas (S.O.)

of data is inadequate. Thus the three curves are superimposed on the single graph to simplify the analysis even though the picture is initially confusing. The rest of the pertinent data are given in Table 2 below. The values given are approximate in most cases, but are adequate to show the feasibility and techniques.

TABLE 2

VARIABLES	TARGETS			
	Open Flame Std. Oil	Natural Gas PG&E	Coal Moapa	Example
Range	950 meters 3120 feet	150 meters 440 feet	210 meters 700 feet	300 meters 1000 feet
Stack Height	30 feet	200 feet	200 feet	---
Plume Depth	1 meter	5 meters	5 meters	5 meters
H_2O in Path	10.8 mm	1.5 mm	2.5 mm	4 mm
Target Temp.	1200 to 1800° F	380° F	320° F	320° F 440° K
Approx. Concentrations				
CO_2 %	9%	9%	17%	13%
H_2O %	18%	18%	6%	12%

The over-all view of the spectra is effected by the temperature of the plumes and the atmospheric attentuation. The effect of atmospheric water vapor is seen in the gap of received energy between 1450 and 1750 cm^{-1}. (Note: to convert wave numbers to microns divide the wave numbers into 10,000) Due to the variation in the amount of water vapor in the line of sight for the three cases, the position of the gap onset and recovery varies the width of the absorption band.

The spectrometer signal strength varied widely in the three cases shown for two reasons. First, the temperature of the open flame was over 1200° F, giving the high frequency end of its curve the highest signal. The middle curve, PG&E's power plant, might be considered typical, while the curve for Nevada Power's Moapa station was low because of energy subtracted with the reference to compensate for the amount of continuum radiation due to ash. More details on the reference effect are below. A further lowering of the

energy for the Moapa curve was due to a uniform degradation of the instrument sensitivity by a factor of about three.

The next most significant features of the three spectra are due to CO_2. The centers of the strongest CO_2 emissions occur at 4.3 microns (2300 cm^{-1}) and at 15 microns (667 cm^{-1}). The atmospheric CO_2 absorbs the center of the associated bands leaving a strong peak on either side. The width of the absorption bands in the center of the emission bands is a function of the range as with the water vapor bands, but is much more consistent due to the fairly uniform distribution of CO_2 in the atmosphere.

The details due to water vapor appear all through the spectra. Because of the large number of occurances of water vapor bands in the spectra, considerable overlap occurs with the bands due to the minor constituents, the pollutants. Thus the details at the high frequency end of the spectrum are due mainly to water vapor in the atmosphere, but are superimposed on the spectra of methane, with at most 2000 ppm. Referring back to the example, in Figure 3 the water vapor emission is shown for 2 mm in a 5 meter plume. At the high frequency end of the spectrum, the energy radiated changes rapidly with temperature, and the open burning plume radiated strongly, the natural gas burning plume, at a lower temperature, radiated moderately, and the coal burning plant radiation was immeasurable, so that the high frequency spectra are subject to considerable variation.

Further details due to the water vapor appear as peaks around 1900 cm^{-1} (5.2 microns) and at 1300 cm^{-1} (7.7 microns). These portions are those skirting the strong water absorption band in between. The band on the 5 micron side overlaps the region for nitric oxide (NO) emission, expected to be the pollutant with the highest concentration in the two upper curves. The curve continues to the edge of the CO_2 band on the high frequency side and continues well into the low frequency region on the other side. The central peak at 1600 cm^{-1} is due to a weak notch in the water spectra, and appears in the example.

On the low frequency side the water vapor contributes most of the energy at the peak and tapers off, providing still important amounts at 1100 cm^{-1} (9 microns). At the peak it obscures the spectra due to small amounts of methane in the natural gas plumes, and obscures the strongest portion of the SO_2 bands in the coal burning plume. Furthermore, it fills in the gaps between the stronger bands thereby reducing the resolution.

The last of the water vapor details appear at 550 cm^{-1} (18 microns) and at 500 cm^{-1}. The first detail is just a notch in the spectra due

to the atmosphere, but it confuses the resolution of the CO_2 and SO_2 spectra occuring at 16.5 and 19 microns, respectively. The latter marks the end of the atmospheric transmission for wavelengths shorter than the bounds of microwaves.

The above accounts for the details of the spectra except for the important region between 800 and 1200 cm^{-1}, (8.35 to 12.5 microns). This region is where the pollutants such as SO_2 are best monitored.

The measurement of the low density pollutants is facillitated by the presence of two weak CO_2 bands at 1060 and 960 cm^{-1} (9.4 and 10.4 microns). The weakness of the bands make their emission equal to that of the adjacent SO_2 band when the density ratio is about 200 to one. Thus with reference to the CO_2 concentration in the above table, the weak pair of peaks at 1160 cm^{-1} next to the CO_2 band at 1040 cm^{-1} indicate about 50 ppm of SO_2 for the PG&E plume, while the lower curve has an order of magnitude more SO_2, 500 ppm, for the coal burning plume.(1) The ratio technique used to obtain the SO_2 levels mentioned above is the essence of this study and is described in detail below.

The ratio technique utilizes the formula,

$$P_s = P_c\,(S_1/S_2)(1/200)$$

where

P_s is the concentration or the partial pressure due to SO_2;

P_c is the concentration of CO_2 which is determined by the nature of the process; e.g., for coal, 15 to 20%;

S_1 is the signal strength received by the spectrometer, in arbitrary, but consistent, units for the SO_2 band at 8.7 microns after the components from superimposed spectra, such as that of water vapor, are subtracted;

S_2 is the signal strength of the CO_2 band at 9.4 microns, taken as above;

and the factor (1/200) is the independently measured relative strength of the SO_2 and CO_2 bands, taken at the appropriate temperature.

As a further check, all of the components are accounted for to be certain that no confusing bands of other constituents appear in the region of calculation. In the preparation of the graphs for calculation, three different curves were used, with one illustrated with the open burning plume and the PG&E plume (Figure 7), one with the components sketched below the curve (Figure 8), and the third used to illustrate the differences due to compensation for the cold sky (Figure 9). All were of the same target, and at the same range, but with differing levels of compensation for the plume opacity. They show the necessity

---

(1) The SO_2 concentration for the S.O. (Standard Oil) curve is ambigious due to spectral overlap.

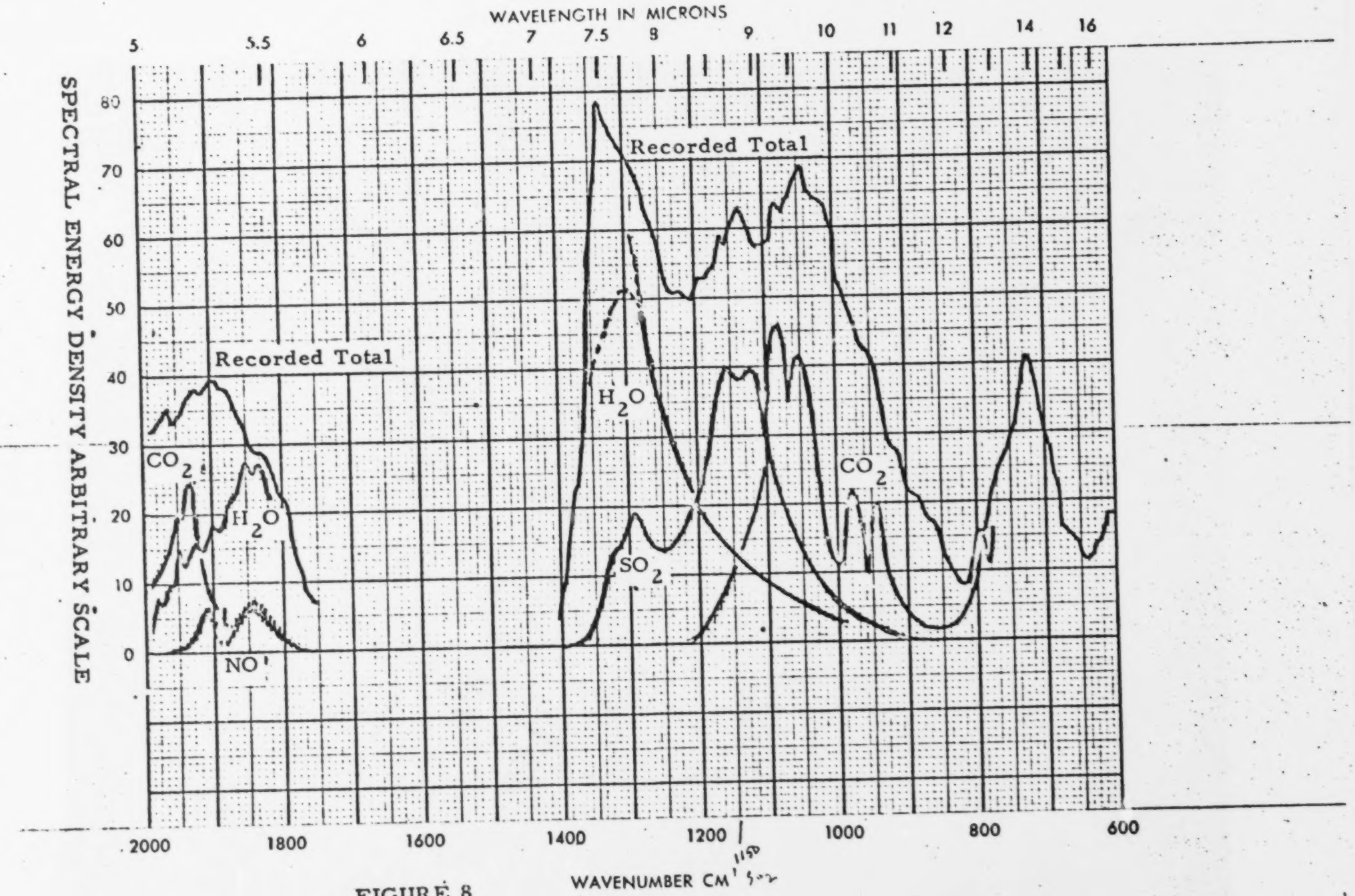

FIGURE 8

Coal Burning Plume Spectrum From Moapa, Nevada
Lower Curves are for the estimated spectral contribution of the gases in the plume.

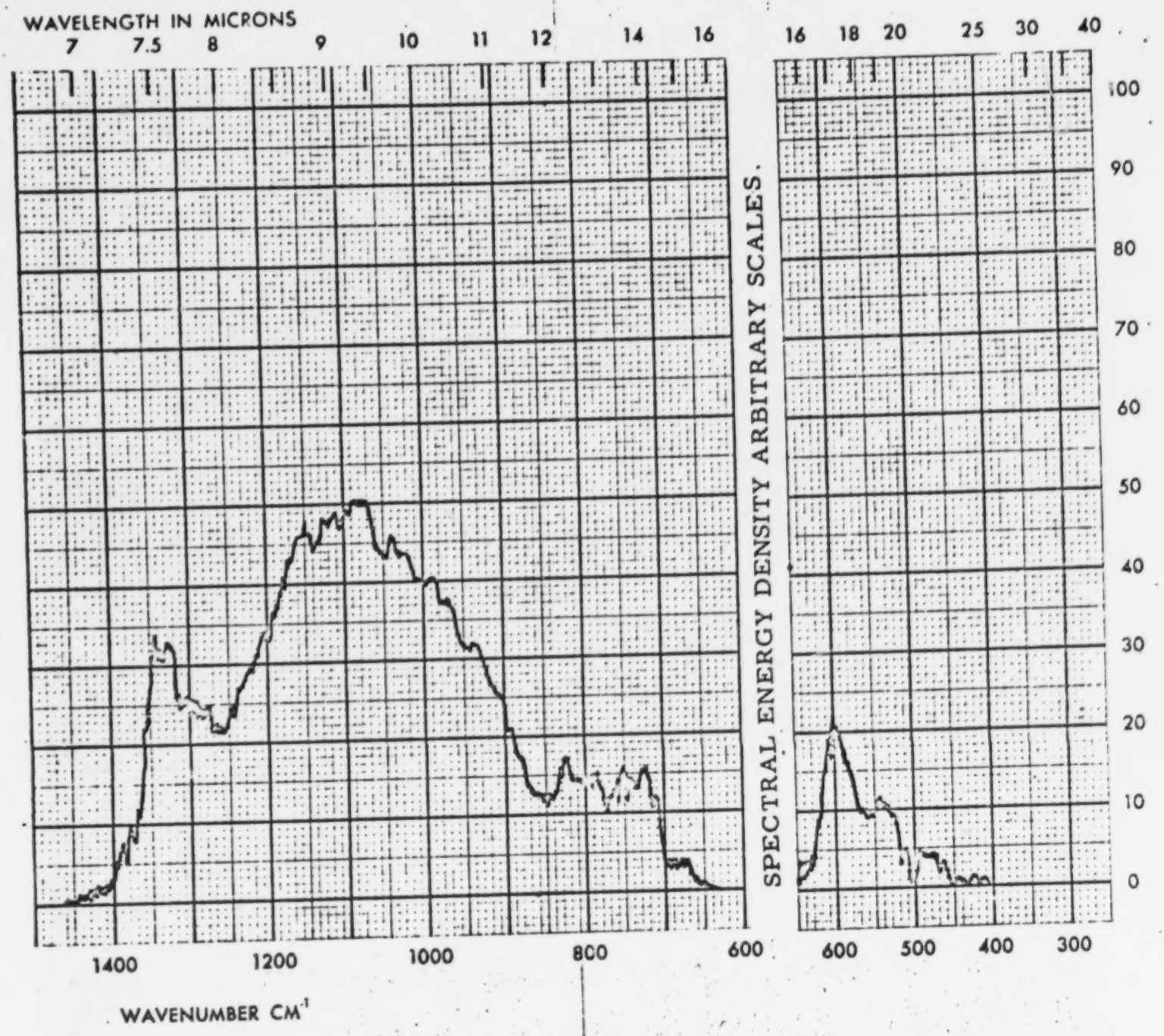

FIGURE 9

Coal Burning Plume with Sky Balance (Moapa)

The analytic and reference beams were balanced to produce zero signal when both were directed into the clear sky adjacent the plume.

of careful application of data reduction techniques. Use of any of the three curves in the calculation gives a concentration varying in the range of 500 to 1000 ppm. In the actual field use of an operational system where legalities would be involved, an accurate measure of the ash content and associated continuum radiation would narrow the range of concentration values to acceptable limits.

Other bands due to pollutants in the plumes are not evident. This is not to say they cannot be found, as is explained in the feasibility section, but with the present instrumentation the energy levels and attendant noise prevented further resolution increases. Other pollutants were found, and are described in the portions below the elaboration of the Moapa spectra.

In Figure 8 the spectra of several runs taken at Moapa are averaged, and the constituents are estimated with the appropriate curves below. The averaging was necessary to compensate for both the effects of the turbulence of the plume and the noise due to an internal loss in signal sensitivity.

Several aspects of the spectrum that are not expected show up on closer analysis. The location of the peak of energy at 7.5 microns occurs nearer the edge of the water vapor absorption region than in the example or in the case of the PG&E natural gas plume where there was more water vapor emission and less absorption. Such a peak is due to two things; first the obvious is the strong SO_2 band at that location, and second, to a skewing of the spectrum. The Moapa station had been on the line only a short time, and did not have the ash content of the plume under control. As a consequence, there was a considerable continuum radiation due to the solid particles in the plume. To decrease their effect and enhance the resolution of emission bands, the reference was biased by obscuring the reference aperture partially. Then the reference was partly to ambient temperature rather than to the cold sky beyond the plume. In Figure 9 the curve is shown with the balance set to zero signal with both the reference and the analytic beam aimed at clear sky. In that curve the band details are lost in the noise level of the spectrometer system.

Such a skewing of the spectrum causes only a small difference in the amount of SO_2 estimated because of the close proximity of the CO_2 reference band, but estimation of the water content would be misleading. Reference to the curve of Figure 4a, taken from the 350' stack of Monsanto company's sulfur burning process in Martinez, California, gives the shape of the SO_2 spectrum with 3.2 mm of water in the path. The shape of that spectrum is the one used in the curve of Figure 8 and indicates that most of the energy at 7.5 microns is due

to the water vapor. But skewing the SO_2 curve to present the total in Figure 8 gives the majority of the radiation to the SO_2. Thus, in comparing the water to the CO_2, the ratio at first appears to be one to one (molecule to molecule) while the ratio with the skewing accounted for gives about 3 CO_2 molecules per H_2O molecule, a figure more typical of coal burning.

Other components of the coal type plume are expected to be NO, CH_3COOH, H_2S, and CO. The amount of NO expected in the plume is shown in the figure, but was not actually resolved. The amount of CH_3COOH in the example, 300 ppm, is evidently too large for the case of the Moapa plume. Such a density would strongly fill in the region between 8 and 8.5 microns. For the amount to not be discernible, a concentration below 100 ppm would be in order. Measurement of the coal quality has not been made, but it is expected that the lignite used (from Spring Canyon mines, Utah) would be higher in organics than the bituminous used for the 300 ppm example. The only data obtained was that the coal contained less than 1% sulfur as confirmed by the low SO_2 concentration observed, and that the ash content was high as shown by the difficulty in suppressing the visible ash plume.

One other pollutant which occurs in the plumes of coal burning operations is H_2S, generally at a level of 1/6 to 1/7 of the SO_2 level. Since the spectrum of H_2S is very weak, it is not expected that 75 ppm of H_2S would show when its strongest region, 7.5 to 8.0 microns, is already emitting due to water, SO_2, etc.

Consider next the curves averaged and shown in Figure 10. These data were taken of the plume from the Tidewater Oil Company's Avon refinery fluid coker. It is evidently the most toxic plume observed in the program.

During the period of the week in which the measurements were made, the coker and associated equipment were in an "upset operation" with one of the processes being bypassed. The obvious components are carbon monoxide, 2050 to 2220 cm^{-1}, CO_2 band edge at 2400 cm^{-1}, middle weight hydrocarbon gases such as n- and iso-butane, 2700 to 3000 cm^{-1} and ammonia with twin peaks at 3300 and 3400 cm^{-1}, and again at 930 and 960 cm^{-1}. A pair of peaks at 2570 and 2630 cm^{-1} are persistent in all the curves and may be due to cyanogen $(CN)_2$, in view of the lack of oxygen and the activity of the nitrogen in the high temperature process.

The cyanogen cannot be confirmed at this time due to the obscuration of the bands necessary to give complete identification. The other bands are at 4.7 microns, confused with CO, and at 13.7 microns, attenuated by atmospheric CO_2. The thickness of the plume, on the order of three meters, and the general shape of the curve, lead one

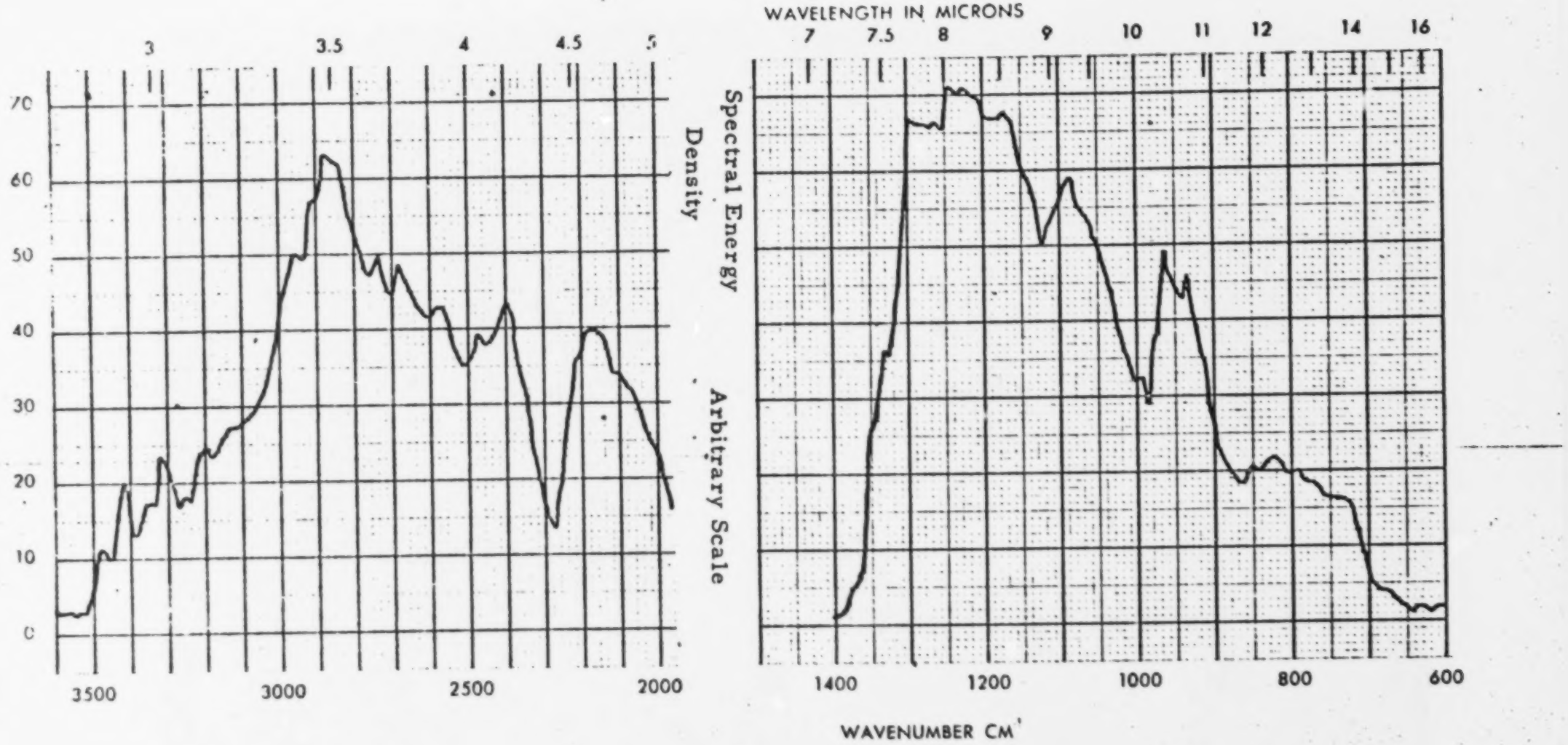

FIGURE 10 Spectral Averages of an Oil Refinery Flume, Tidewater at Avon. Full-scale-limited and absent portions of spectra not included in averaging sum, and the divisor was chosen to suit. Six to ten curves were used. The scales of the high frequency section and low frequency section are not the same. The region from 2500 to 2700 cm^{-1} was about 50% lower than shown for the curves made the previous week, but the (CN_2) peaks were still present.

to expect that the emissivity of the plume is near one at several wavelengths, particularly in the 3.5, 4.7, 8.0 and 10.5 micron regions.

The CO density has been measured at around 8% which, by referring to the curves given by Penner[2], would give a low resolution emissivity of approximately 70% at 4.7 micron fundamental. The resulting 8 atm-cm of CO (assuming 8% of the one meter effective path length) will result in the individual lines of the band to be completely opaque with an emissivity of one. The resultant non-linearity of the absorptivity in the spaces between the lines makes the absorption function too complex to use as a reference band. However, the shape of the NH_3 curve brackets its density by virtue of the broad bands to either side of the 900 and 1000 cm^{-1} (10 and 9 micron) band edges. The resultant density for a three meter plume puts the NH_3 in the 1000 to 10,000 ppm range. Such an estimate is one to two orders of magnitude higher than the estimate of the Bay Area Air Pollution Control District. Further resolution of this disparity is precluded by time.

The estimate for the cyanogen content based on the two band peaks noted is similar to the NH_3. The two gases are presumably due to the same high temperature reduction process, so resolution of the NH3 density problem would probably affect the cyanogen estimate as well.

A summary, then, of the quantitative analysis using the ratio and band distortion techniques yields the following data:

	SO_2	CO	NH_3	$(CN)_2$
1. MOAPA (coal burning)	500 ppm	1000 ppm	---	---
2. PG&E (natural gas)	50	300	100	100
3. Tidewater (petroleum products)	1000-3000	8%	1000-10,000	1000

3. SOME LIMITATIONS ON FEASIBILITY

Since it is obvious from all the preceding that the gross measurements are feasible, the matter at hand is the degree of sensitivity and accuracy, and the adequacy of the measurements for the pollution problem solution.

The limits of measurement encountered in this work are described below, while their applicability will depend upon the user agency. These limits may be placed in three categories; (1) limits due to the nature of the plume and its constituents, (2) environment and circum-

(2) Quantitative Molecular Spectroscopy and Gas Emissivities - S. S. Penner - Addison-Wesley Publishing Company, Inc. - 1959

stances, and (3) the equipment.

The limits of plume constituent determinations result when the combination of bands viewed overlaps to the degree that separation is difficult, continuum radiation upsets the background balancing or optical depth is only a fraction of the plume depth with the associated distortion or elimination of band details.

a. Limits due to Plume Constituents. Overlap of bands in the spectra cause confusion or obscuration of the plume components. A short table (Table 3) is given illustrating the limits for the cases of three combustion product examples, oxidizing hydrogen, carbon or both. The examples do not give the limit as an absolute measure since that can vary with curtain analytical techniques, such as cross correlation (use of a sample gas as a filter), or fine structure analysis.

TABLE 3

DETECTION LIMITS DUE TO SPECTRAL OVERLAP BY PRIMARY EXHAUST PRODUCTS

The limits given below occur when the emissivity of the pollutant is equal to that of the CO_2 and H_2O at the identifying band.

			Methane CH_4 9.1% CO_2 18.2% H_2O		Heavy Oil -CH_2- 12.5% CO_2 12.5% H_2O		Coal 16.7% CO_2 5.6% H_2O	
Pollutant	Identifying Band cm^{-1}	cm Path for Emissivity = 0.1	Concentration Limit ppm	Emissivity at 1 meter Limit ppm	ppm	Emissivity	ppm	Emissivity
SO_2	1350	.0263	410	150×10^{-3}	290	110×10^{-3}	130	49×10^{-3}
	1150	.10	7.2	$.72\times10^{-3}$	5.0	$.5\times10^{-3}$	2.2	$.22\times10^{-3}$
	520	.30	136	4.5×10^{-3}	188	6.3×10^{-3}	250	8.3×10^{-3}
NO	1850	.632	6%	0.66	4%	0.49	1.85%	0.27
NO_2	1280	.033	44	13×10^{-3}	31	9.4×10^{-3}	13	3.9×10^{-3}
	750	.055	1450	260×10^{-3}	2000	360×10^{-3}	2700	490×10^{-3}
CO	2150	.09	117	13×10^{-3}	103	11×10^{-3}	84	9.3×10^{-3}
NH_3	960-930	.316	270	8.5×10^{-3}	380	12×10^{-3}	500	15.8×10^{-3}
H_2S	1220-1350	6.70	1280	1.9×10^{-3}	890	1.3×10^{-3}	400	0.6×10^{-3}
$(CN)_2$	2650	2.30	156	0.68×10^{-3}	165	$.72\times10^{-3}$	176	$.76\times10^{-3}$
	2520	2.30	867	3.8×10^{-3}	1169	5.1×10^{-3}	1548	6.7×10^{-3}
	2150	.03	39	13×10^{-3}	33	11×10^{-3}	27	9×10^{-3}
CH_3COOH	1200	.020	3.8	1.9×10^{-3}	2.6	1.3×10^{-3}	1.1	0.55×10^{-3}
	550	.088	40	4.5×10^{-3}	55	6.2×10^{-3}	74	8.4×10^{-3}
$CH_2{:}CH_2$	950	.055	50	0.91×10^{-3}	69	1.3×10^{-3}	92	1.7×10^{-3}

COMMENTS ON TABLE 3

The calculations in the above table are based on the assumption that detection is limited when the emissivity of a major constituent of the observed plume is equal to the emissivity of the pollutant sought at the identifying band(s) of the pollutant. Variations in practice are considerable, however, and depend further on the presence of multiple pollutants. In some cases more than one band is available for measurement, but for di-atomic gases such as NO, CO and HCl, only one fundamental is available and the harmonics frequently obscured (as with NO whose first overtone is confused with the 2.7 micron water band) as well as being at a high frequency where there is little energy in a plume of typical temperature.

To calculate the major constituents of the plumes used in the above table simple chemistry was used, assuming complete combustion to CO_2 and H_2O. For the heavy oil case, the hydrogen on the end of the carbon chains was ignored and a formula CH_2 was used. Since in the case of coal burning the amount of water in the plume varies considerably, a simple ratio of three CO_2 to one H_2O was assumed as a typical example.

The lower limit of detectivity occurs for an emissivity of the order of 10^{-3} when the band being studied lies near the center of the blackbody curve for a plume of, say, 200° F or more. Using the optical system outlined in this section, the received energy is on the order of 10^{-9} watts for a 1/2 micron bandwidth at 8 microns. A minimum sensitivity of 10^{-9} watts is typical of modern radiometry. Therefore, if the emissivity given in the table is less than 1x10-3, it is unlikely that the limit given will be realized without more than one meter of plume to sight through.

The one meter path was chosen to simplify calculation; other path lengths simply result in proportional increases in the emissivity for those cases where the emissivity is less than 100x10-3. The NO appears at such a high density that the calculations are all exponential. With reference to the section on line width, it should be noted that NO has a distinct line structure and should be handled with the strong line approximation when detailed calculations are made at the concentrations shown.

The actual detection limit encountered in the field depends on a large number of parameters. The table above gives the limits due to obscuration of just two components of the plume. If some of the pollutants are present in large amounts, further obscuration will occur. Furthermore, even if other obscurations do not occur, the limiting concentration may not allow enough energy to be emitted in a reasonable sized plume. Thus the emissivity for one meter (3.28') of plume depth at the related density is given for each of the bands for each of the fuels. Other variations in the application of the limits occur when the obscuring spectrum is of grossly different shape than the one sought. In the case of SO_2 and water at 1150 cm^{-1} (8.7 microns) the SO_2 stands out against a smooth background, while in the case of NO and water at 1900 cm^{-1} (5.3 microns) the water vapor details are so coarse as to obscure any details due to NO when the NO emissivity is equal

COMMENTS ON TABLE 3 R-3159-3954

to that of the water. However, more careful measurement of the details than was done in this feasibility study could improve the NO detection limit.

The calculations are approximate to the purpose of feasibility illustration. For field work the nature of the specific analytical technique can make significant differences in either the improvement or decrement of resolution. Also, the accuracy would be improved with more accurate measure of emissivity as a function of temperature. In particular, the emissivity of acetic acid varies considerably with temperature due to dimerization (pairing of the molecules by hydrogen bonding). For the calculations above the emissivity was taken from spectra run at approximately the same temperature, 300°F.

COMMENTS ON TABLE 3 (cont'd) R-3159-3954

b. Limits due to Environment. The weather and the range-to-target are parameters used in a product form to predict the atmospheric obscuration.

The maximum allowed water in the path divided by the water vapor density yields the maximum range under the prevailing weather. This is illustrated in Figure 11 where the range is plotted as a function of dew point (a common measure of the absolute humidity), and the range is given for two common limits, 1 mm, and 5 mm of precipitable water. Actual precipitation of water vapor (when the ambient temperature reaches the dew point) causes scattering of the energy and the limits associated with eyeball visibility are then suitable for the spectrometer limits.

c. Limits due to Equipment. Range limitations due to the geometry of the measurements will be a function of the aperture of the optical system, the detector size and the f-number (as with the f-number denoting efficiency of a camera). If the optical system is set up so that the target always fills the field of view for any reasonable target size, then the energy density on the detector will only be a function of the atmospheric attenuation. This is of great value in keeping the dynamic range requirements small. The following is an example of the values found by maximizing signal to the point where other parameters begin to dominate, i.e., a typical compromise:

f-number (focal length, F, divided by aperture)	2.0	limited by cost of optics
aperture	8.0"	limited by portability
IR detector size (d)	1 mm	balance between state of the art of IR detectors and field of view, θ
Field of View θ	8.4 minutes	equal to 2.44 feet at a range of 1000 feet

$$\theta = \tan^{-1}\frac{d}{F}$$

$$f = \frac{F}{A} = 2$$

$$F = 2 \times 8" = 16"$$

R-3159-3954

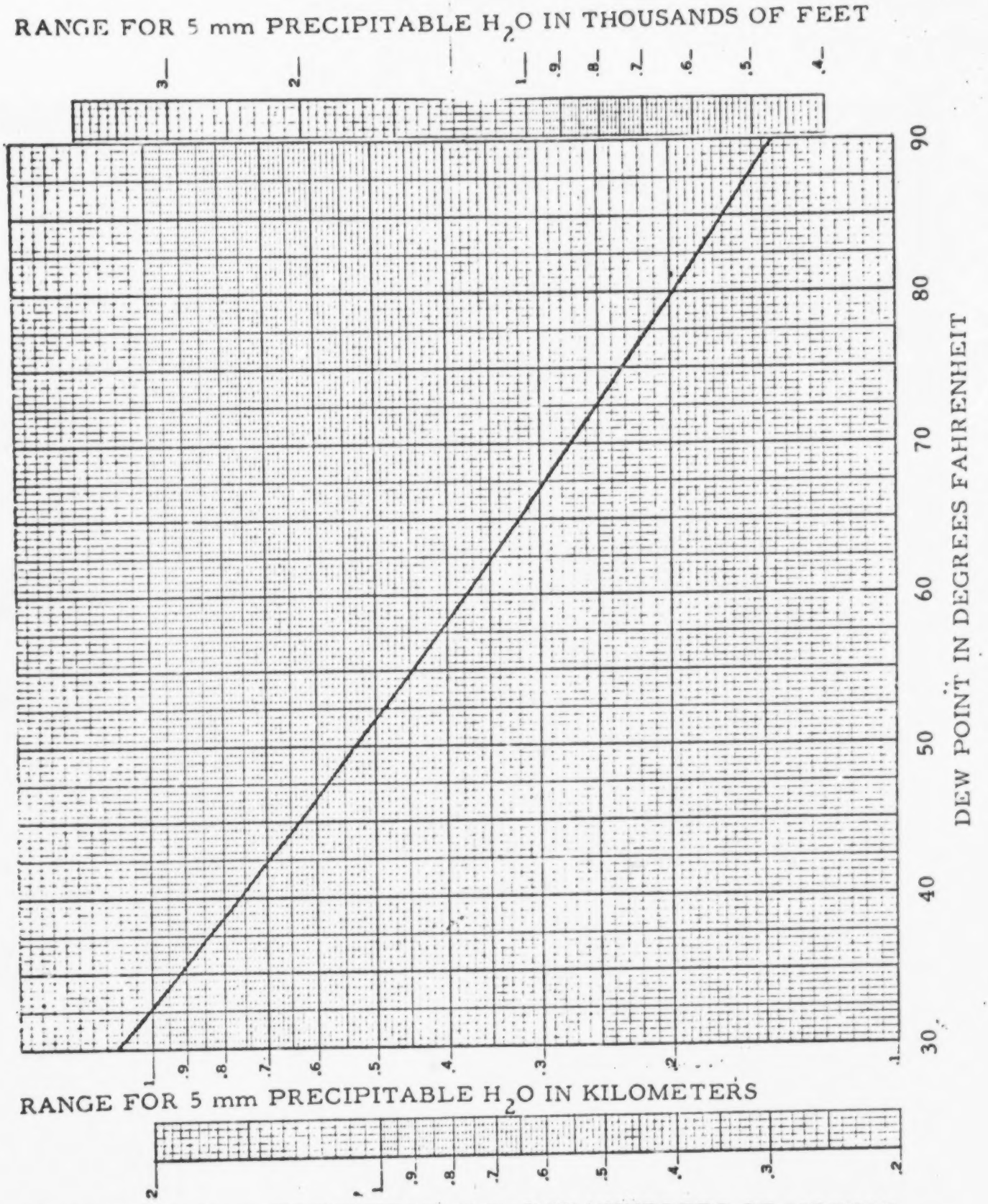

FIGURE 11

RANGE DUE TO ATMOSPHERIC WATER VAPOR

SECTION VII

CONCLUSION

Passive pollution source monitoring has both political and economic advantages. These advantages may be realized through a spectrally selective radiometer. This report has demonstrated the effectiveness of a simple commercial spectrometer combined with telescopic operation. The resulting instrument was an adaptation rather than an original design. Effectiveness was limited to the degree of time consuming analysis expended with each target.

The limit of accuracy was set by the amount of time and equipment involved in this short study, rather than by the nature of the spectrographic analysis method.

The complexity of spectral analysis indicates a requirement of automatic data reduction within the instrument as part of a passive analysis system design. Any phenomonon is complex when studied in depth. The complexity is dependent upon the relative significance of the parameters describing a phenomonon, and the facility with which the relationship of the parameters may be expressed. That is, how many variables are in the formula, and does the formula admit to a closed form of solution, or acceptable approximations. Considering the number of variables of major significance, and the exponential nature of the associated formulae, analytical solutions of frequency selective energy transfer, with quantitative identification of sources is a complex problem facing the analyst. However, by noting the analogy that one may eat food and digest it successfully without a computational expose' of the digestive processes, one may reasonably expect to find suitable natural processes to do portions of the emissivity analysis. For example, it was noted that the fine structure of nitric oxide would suffice to separate it from the overlapping water vapor emissions from some plumes. Simply improving the resolution of a dispersive instrument would not be adequate because of the consequent loss of energy to the system. However, placing a sample of the gas under analysis in the beam of the instrument results in an interaction of the fine structure of the absorbing sample and the emitting source. This interaction is an attenuation different from that of a neutral (spectrally uniform) attenuator, and could be referenced to controlled experimental measurement.

The point of the above is that the exposition in the previous sections is necessary to describe the process, but actual performance of such measurement may be much more direct, and be significantly less time consuming, when using suitably designed instruments.

Proper design will depend on the user agencies specific needs; but two general categories of instrument may be considered: a simple two-gas-ratio instrument for specific analysis, or a general purpose instrument with the flexibility to uncover new pollution problems, and act as either a passive or active signal processor.

It is strongly recommended that a passive infrared instrument designed specifically to measure one or two stack pollutants be constructed and evaluated under actual user conditions. In particular, tests performed during this contract indicate that a quantitative SO_2 monitor will be effective under many typical conditions. As discussed in Section VI this instrument would obtain its basic information by computing the ratio of SO_2 emission at 8.7 microns and CO_2 emission at 9.4 microns. Suitable data processing circuitry will convert this ratio into SO_2 concentration that can be read by a relatively unskilled operator. Detailed field tests with such an instrument should yield data concerning its accuracy under various conditions (using "in place" samples as a reference), its sensitivity and dynamic range, the limiting geometrical and environmental conditions, and the effectiveness of the man-machine interface. These field test results can then be constructively used to improve the effectiveness of the SO_2 monitor and/or used to design instruments that can monitor pollutants other than SO_2.

SECTION VIII

APPENDIX

1.. Spectrum Index

Below is a listing of all the spectrographs made in the course of the Robert Taft Sanitary Engineering Center contract for infrared study of industrial stack plumes. The significant spectra of the series have all been submitted in the monthly reports. These spectra have the various signal gain scale factors noted on them; however it should be noted that due to the blaze angle of the gratings, the efficiency of the orders, and the interference filters used within the instrument, there is an increase in the effective gain of 15 when the instrument goes from the high frequency section to the center section, and an increase of 5 when the insttument goes from the center section to the low frequency section.

The notations with the spectral listings are:

Quality - - a measure of the degree with which the experiment was successful, not the overall appearance --

Absorption of Emission -- since both occur in any of the experiments, the reference generally is to the relative temperature of subject under analysis --

Double or Single Beam -- normally refers to the use of the servo-attenuator within the instrument; however, since the instrument always operates with both an analytic and reference beam, the symbol used indicates the importance of reference beam: for single beam notation the reference energy was neglible --

Telescopic -- the T notes when the analytic beam was focused at infinity by optics external to the spectrometer --

Resolution --indicates whether or not the spectrometer slit width was controlled by the internal cam (Ni) or was opened to a fixed lower resolution (lo).

IR-10 SPECTROGRAPH INDEX

NUMBER	SUBJECT	QUALITY G Good F Fair P Poor	ABSORPTION OR EMISSION A or E	DOUBLE-BEAM OR SINGLE D or S	TELESCOPIC T	RESOLUTION HI or LO
1	Air (6' Path internal to Spectmtr)	G	A	S		HI
2	Inst. Test Air	P	A	S, D		LO
3	Soldering Iron at 40', air	F	A	S	T	LO 2mm
4	Soldering Iron at 40'	P	A	S	T	LO
5	Sky at Zenith	P	E	S	T	LO
6	Soldering Iron at 40'	P	A	S	T	LO
7	" " " "	G	A	S	T	LO
8	" " " "	P	A	S	T	LO
9	" " " "	P	A	S	T	LO
10	" " " "	P	A	S	T	LO
11	Horizon from Roof	P	E	S	T	LO
12	" " "	P	E	S	T	LO
13	" " "	P	E	S	T	LO
14	Roof Top Stacks	P	E	S	T	LO
15	DV Plastics Oven Stack	P	E	S	T	LO
16	CO_2 and SO_2	P	A	S		LO
17	" " "	F	A	S		LO
18	CO_2 and SO_2 Resolution Test	G	A	S		LO
19	$SO_2 + CO_2$ 10 cm Salt Windows	G	A	D		HI
20	$SO_2 + CO_2$ in Hot Beaker, Poly Window	P	A	S		LO
21A	Inst. Test, Gain vs. Resolution	G	A	S		LO

R-3159-3954

NUMBER	SUBJECT	QUALITY G Good F Fair P Poor	ABSORPTION OR EMISSION A or E	DOUBLE-BEAM OR SINGLE D or S	TELESCOPIC T	RESOLUTION HI or LO
21B	Inst. Test Slit vs. SB%	G	A	S		LO
21C	Inst. Test SB% & Bal.	G	A	S		LO
21D	Inst. Test Varied SB% at 1 mm	F	A	S		LO
21E	Inst. Test Listing for SB Gain Schedule		A	S		LO
22A	Hot SO_2 & CO_2 in Beaker with Poly Window	G	E	S		LO
22B	"	G	E	S		LO
23	Inst. Test w/modified comb -magnifies low ABS details	G	A	D		HI
24	Black Body Ref. Curves (sketched)	G	E			
25A	Fixed Air (NO_2)	G	E	S		LO
25B	Fixed Air	G	E	S		LO
26A	SO_2 in 3' Tank, Short Path	F	E	S		LO
26B	"	G	E	S		LO
27	Polyethylene, 1/2 mil and 2 mil	G	A	D		HI
28	"	G	A	S		LO
29	"	F	A	D		LO
30	Acetone Emission, 3' Tank w/Poly Windows	G	E	S	T	LO
31A	SO_2 in NaCl 10 cm cell, Varied Density	G	A	D		HI
31B	"	G	A	D		HI
32	1st Cold Reference Tests - Sky	G	E	D	T	LO
33	Cold Ref. Test Horizon	F	E	D	T	LO

ROBERT TAFT ENG. CENTER SERIES

IR-10 SPECTROGRAPH INDEX

NUMBER	SUBJECT	QUALITY G Good F Fair P Poor	ABSORPTION OR EMISSION A or E	DOUBLE-BEAM OR SINGLE D or S	TELESCOPIC T	RESOLUTION HI or LO
34	Cold Ref. Test Horizon	P	E	D	T	LO
35	Dry Ice Ref., Horizon	G	E	D	T	LO
36	Dry Ice Ref., Horizon	G	E	D	T	LO
36A	Dry Ice Transmission	P	A	D		HI
37	CO_2 vs. Carboard	F		D		LO
38	CO_2 & Ref. Can Comparison	G	E	D		LO
39	Cold Ref. Scans (4) at SB 30, 50, 60, 70	G	E	D	T	LO
40	Emissivity of Solid CO_2	G	E	D		LO
41	Ref. Mirror Balancing	F	E	D	T	LO
42	Bayside Oil Co. Stack	P	E	D	T	LO
42A	Sky at SB76, Full Ref.	G	E	D	T	LO
43	Fiberglas Co. Santa Clara	P	E	D	T	LO
44	" (Sky)	F	E	D	T	LO
45	McCauley Foundry (scrap metal)	F	E	D	T	LO
46	"	F	E	D	T	LO
47	Std. Oil Co. Background Runs			D	T	LO
48	Std. Oil - Inst. Malfunction					
49	Std. Oil, Stack Group (6) No stack emission noted.	F	E	D	T	LO

ROBERT TAFT ENG. CENTER SERIES

IR-10 SPECTROGRAPH INDEX

NUMBER	SUBJECT	QUALITY G Good F Fair P Poor	ABSORPTION OR EMISSION A or E	DOUBLE-BEAM OR SINGLE D or S	TELESCOPIC T	RESOLUTION HI or LO
50	Std. Oil, (6), some features of long range H_2O, CO_2	P	E	D	T	LO
51	Std. Oil (6) Hot Continuum (Stack)	F	E	D	T	LO
52	Richmond Smog, Cold Ref. (see #39)	F	E	D	T	LO
53	Solar Spectrum	F	E	S	T	HI
54	Solar Spectrum	G	E	S	T	HI
55	Std. Oil, 1 km Ref. Run	F	E	D	T	LO
56	Std. Oil, Gas Burn-off Tower 950 Metal Range	G	E	D	T	LO
57	Test Tank, 18", CO_2 at 155°F	F	E	D	T	LO
58	" " " " at 165°F	G	E	D	T	LO
59	" " " " at 175°F					
60	CO_2 + SO_2 in Test Tank	F	E	D	T	LO
61	CO_2 in Test Tank at 125' 183°F	F	E	D	T	LO
62	SO_2 Emission in Test Tank (w/CO_2)	F	E	D	T	LO
63	Air-CO_2-SO_2 1:0.17:0.001 140 - 160F 1:1/6:1/1000	F	E	D	T	LO
64	" at 180-200F	F	E	D	T	LO
65	"	P	E	D	T	LO
66	SO_2 Emission w/weak CO_2	F	E	D	T	LO

ROBERT TAFT ENG. CENTER SERIES

IR-10 SPECTROGRAPH INDEX

NUMBER	SUBJECT	QUALITY G Good F Fair P Poor	ABSORPTION OR EMISSION A or E	DOUBLE-BEAM OR SINGLE D or S	TELESCOPIC T	RESOLUTION HI or LO
67	Air:CO_2:SO_2 1:1/6:1/1000 90 yards	P	E	D	T	LO
68	" 47 yards	P	E	D	T	LO
69	Ideal Cement (Opaque Steam Plume)	P	E	D	T	LO
70	CO_2 in Test Tank at 95 yards	P	E	D	T	LO
71	Hunters Point PG&E Steam/ Elect. 200' Stack	G	E	D	T	LO
72	Hunters Pt. 250' Stack, 2 ranges of 150 meters & 300 meters.	G	E	D	T	LO
73	" at 300 meters	F	E	D	T	LO
74	CO_2 Test Tank 145' 190°F	F	E	D	T	LO
75	SARAN	G	A	D		HI
76	SO_2 Emission 230F at 145'	G	E	D	T	LO
77	SO_2 and CO_2 at 145', 240°F	G	E	D	T	LO
78	SO_2 and CO_2 at 250°F	G	E	D	T	LO
79	SO_2 and CO_2 vs. CO_2 190°F	F	E	D	T	LO
80	CO_2 in Test Chamber 245°F	G	E	D	T	LO
81	Hunters Point PG&E 200' Stack 150M	G	E	D	T	LO
82	"	G				
83	Steam in Test Tank at 212F	F	E	D	T	LO
84	Hunters Point PG&E Aimed at Stack	F	E	D	T	LO

ROBERT TAFT ENG. CENTER SERIES

IR-10 SPECTROGRAPH INDEX

NUMBER	SUBJECT	QUALITY G Good F Fair P Poor	ABSORPTION OR EMISSION A or E	DOUBLE-BEAM OR SINGLE D or S	TELESCOPIC T	RESOLUTION HI or LO
85	Hunters Point PG&E Aimed at Stack Large Variation Due to Wind on Solid Target	F	E	D	T	LO
86	Hunters Point 250' Plume	G	E	D	T	LO
87	Hunters Point 250' Stack	G	E	D	T	LO
88	Tidewater Oil Co. Fluid Coker Stack	G	E	D	T	LO
89	"	G	E	D	T	LO
90	Monsanto 250' SO_2 Vent	F	E	D	T	LO
91	"	G	E	D	T	LO
92	"	G	E	D	T	LO
93	Tidewater Coker at 115 Meters	G	E	D	T	LO
94	", 115m various elevations					
95	" ,115 m & 250 M					
96	" ,380 m & 460 M					
97	Nevada Power at Moapa, Coal	P	E	D	T	LO
98	"	F				
99	" , 250M	F				
100	"	P				
101	"	G				
102	", clear sky bal.	G				
103	"	F				
104	", good balance	G				

ROBERT TAFT ENG. CENTER SERIES

IR-10 SPECTROGRAPH INDEX

NUMBER	SUBJECT	QUALITY G Good F Fair P Poor	ABSORPTION OR EMISSION A or E	DOUBLE-BEAM OR SINGLE D or S	TELESCOPIC T	RESOLUTION HI or LO
105 - 110	Hot H_2O-Hydrogen Flame 8" Test Flue	F	E	D	T	LO
111	Globar Thru 10^4 inches Atmosphere (833-1/3 Feet) Between DV Towers	F	E	D	T	LO

APPENDIX

SO_2 DATA

Although there is much data available on the spectroscopic constants of H_2O and CO_2, SO_2 data is rather sparse; thus the detail calculation constants are given here. The data is from "The Infrared Spectrum and Molecular Constants of Sulfur Dioxide", R. D. Shelton, A. H. Nielsen, W. H. Fletcher, Journal of Physical Chemistry, 21 2178 '53.

Application of the constants may be found in Infrared and Raman Spectra, G. Herzberg, Van Nostrand Co. 1945, p44f. and p469f.

Molecular form: asymetric top rotator nearly prolate spherical) O-S-O with 119.53° included angle and 1.432 Å SPACING.

Moments of Inertia:

$a = 13.8046 \times 10^{-40}$ g cm^2

$b = 81.3067 \times 10^{-40}$

$c = 95.3376 \times 10^{-40}$

Type A bands have Q branches with 0.62 cm^{-1} spacing(ν_3) and type B bands have Q branches with 3.4 cm^{-1} spacing. The close in P and R branches with each Q give the fine structure and effective spacing of 3.54 cm^{-1} (ν_1, ν_2).

3. CONVERSION OF UNITS

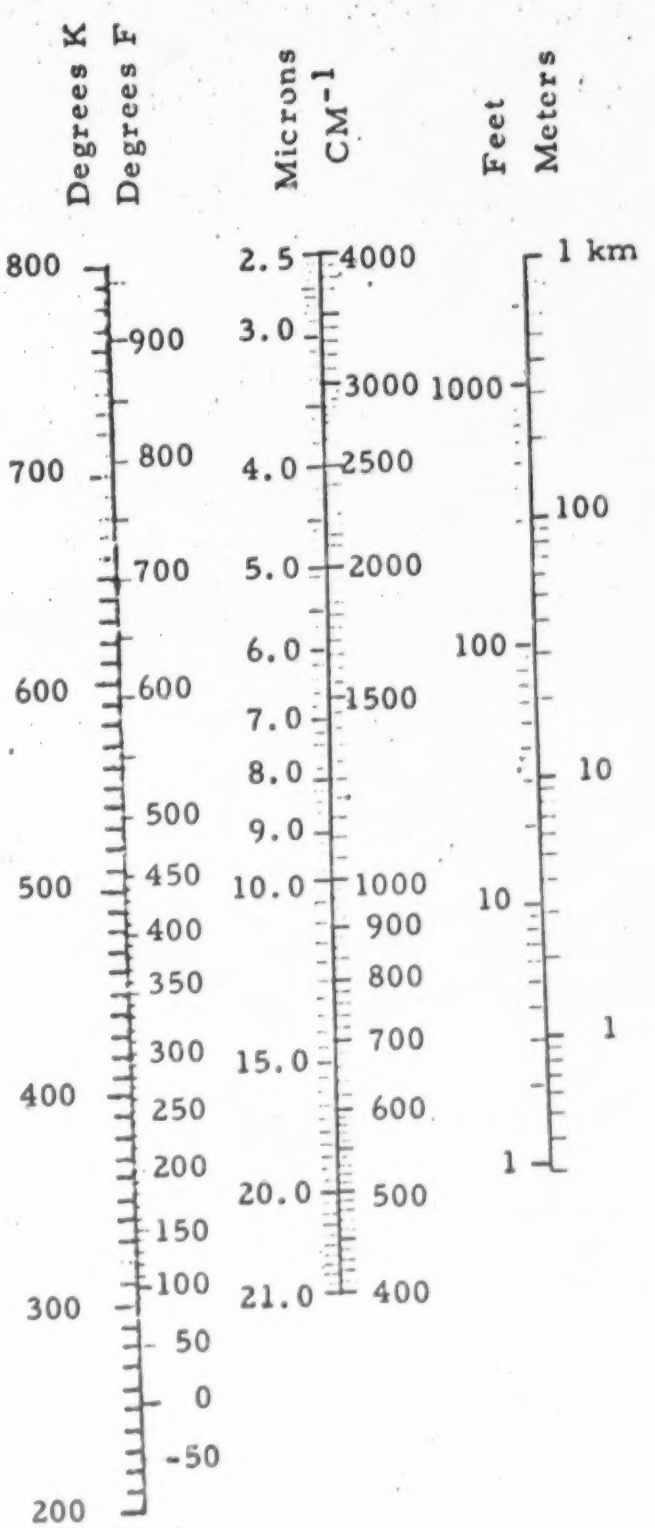

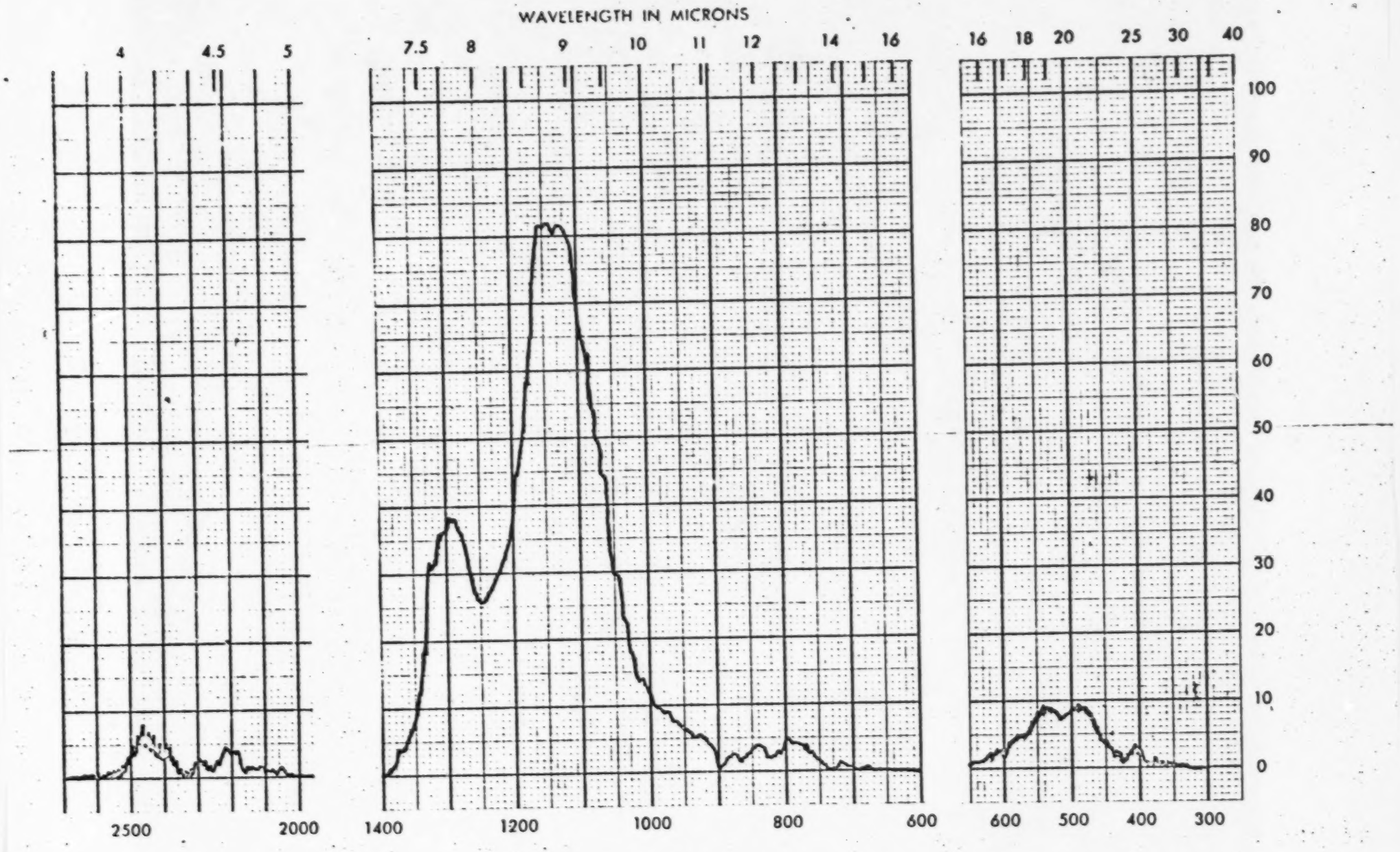

4a. SO_2 emission from 350' double stack at Monsanto Co, Avon. Range approx. 350 meters with dew point at 50° F and clear sky background.

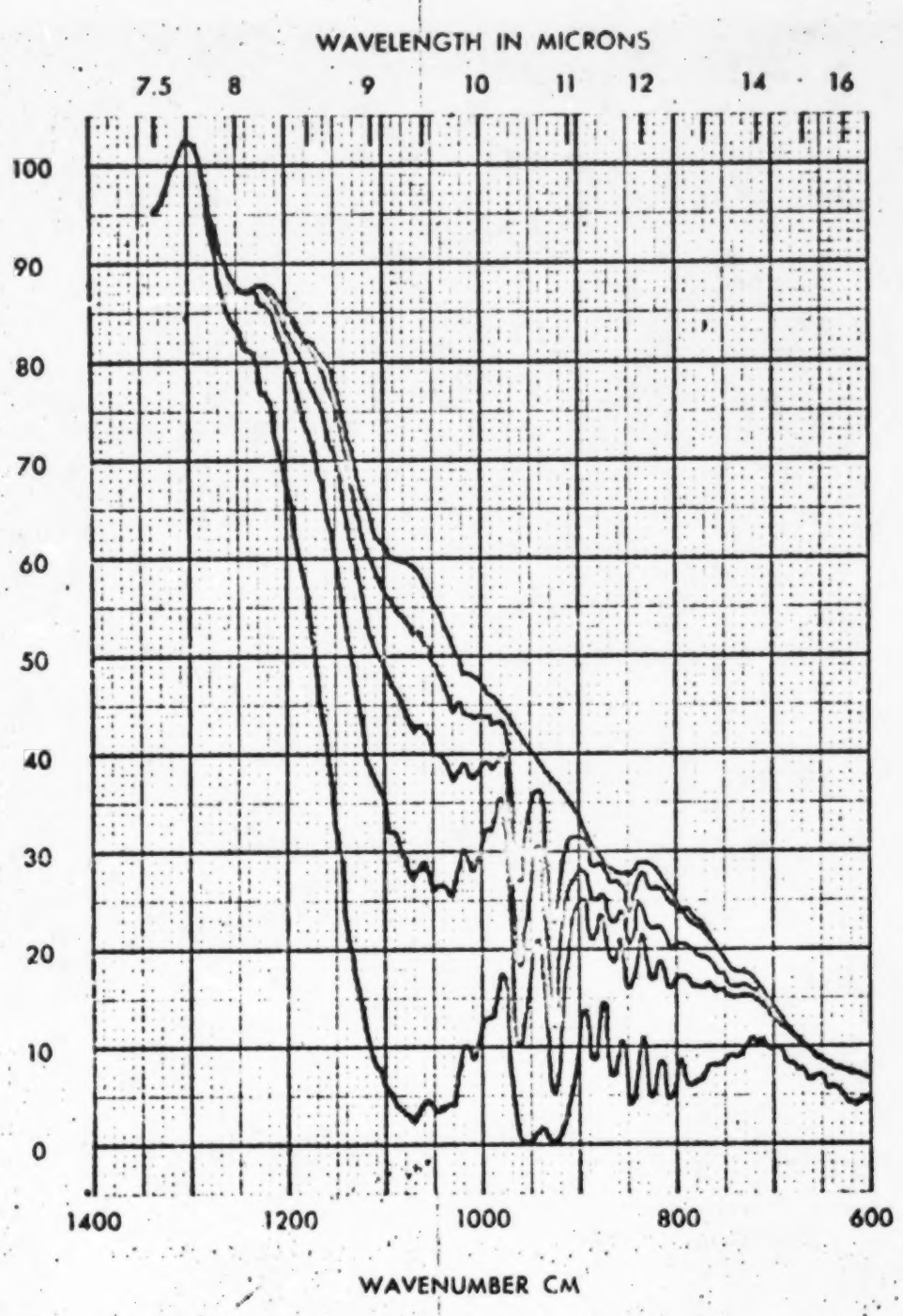

4b. Ammonia, NH_3, on IR 10 with 10 cm cell, max. slit width, single beam operation. Partial pressure of NH_3 reduced in 50% steps. Upper trace is for air only in the cell. All curves at atmospheric pressure.